

## Research Article

# Kinematic and Dynamic Characteristics of the Free-Floating Space Manipulator with Free-Swinging Joint Failure

Qingxuan Jia, Bonan Yuan , Gang Chen , and Yingzhuo Fu 

*School of Automation, Beijing University of Posts and Telecommunications, Beijing 100876, China*

Correspondence should be addressed to Gang Chen; [buptcg@163.com](mailto:buptcg@163.com)

Received 19 June 2019; Revised 29 July 2019; Accepted 8 August 2019; Published 12 September 2019

Academic Editor: Franco Bernelli-Zazzera

Copyright © 2019 Qingxuan Jia et al. This is an open access article distributed under the Creative Commons Attribution License, which permits unrestricted use, distribution, and reproduction in any medium, provided the original work is properly cited.

For the free-floating space manipulator with free-swinging joint failure, motions among its active joints, passive joints, free-floating base, and end-effector are coupled. It is significant to make clear all motion coupling relationships, which are defined as “kinematic coupling relationships” and “dynamic coupling relationships,” inside the system. With the help of conservation of system momentum, the kinematic model is established, and velocity mapping relation between active joints and passive joints, velocity mapping relation between active joints and base, velocity mapping relation between active joints and end-effector. We establish the dynamic model based on the Lagrange equation, and the system inertia matrix is partitioned according to the distribution of active joints, passive joints, and the base. Then, kinematic and dynamic coupling relationships are explicitly derived, and coupling indexes are defined to depict coupling degree. Motions of a space manipulator with free-swinging joint failure simultaneously satisfy the first-order nonholonomic constraint (kinematic coupling relationships) and the second-order nonholonomic constraint (dynamic coupling relationships), and the manipulator can perform tasks through motion planning and control. Finally, simulation experiments are carried out to verify the existence and correctness of the first-order and second-order nonholonomic constraints and display task execution effects of the space manipulator. This research analyzes the kinematic and dynamic characteristics of the free-floating space manipulator with free-swinging joint failure for the first time. It is the theoretical basis of free-swinging joint failure treatment for a space manipulator.

## 1. Introduction

The application of a space manipulator can not only improve execution efficiency of space tasks but also decrease risks of an astronaut's EVA. Therefore, space manipulators play an important role in space exploration [1, 2]. However, space manipulators are exposed to hazardous space environment with high temperature difference and intense radiation and usually execute many heavy tasks, like carrying a load whose mass reaches up to 8-25 tons, so parts in joints suffer from severe abrasion, and joints are prone to fail during the long-term service [3]. Subjected to hazardous environment, maintaining fault joints in orbit is accompanied with high costs and risks, so we hope to design a failure treatment strategy to keep using space manipulators after joint failure [4, 5].

Wu et al. [6] divided joint failure of space manipulators into two types: a fail-on type with infinite torque and a fail-

off type with zero torque, according to joint failure cases in Canadarm1. Afterwards, these two failure types are explicitly defined as locked joint failure and free-swinging joint failure [7, 8]. Locked joint failure means the fault joint is rigidly locked so long as the abnormal operation is detected. Reconfiguring the kinematic and dynamic models, the space manipulator with locked joints is degraded into a new manipulator with less degrees of freedom (DOF) to be used [9, 10]. Free-swinging joints cannot support torque at all, so they swing freely. It is usually caused by motor excitation loss, gear engagement separation, or cracking of the transmission shaft in alternant speed-up and speed-down. However, there are few researches on free-swinging joint failure treatment for space manipulators [11].

For the space manipulator with free-swinging joint failure, its DOF is larger than the number of actuated joints, so it is an underactuated system. Referring to the service

experience of underactuated manipulators on the ground, we conclude that free-swinging joint failure treatment methods mainly include the following: (1) direct control of underactuated manipulators to execute tasks [12]; (2) with the help of the kinematic and dynamic coupling relationships between active joints and passive joints, free-swinging joints are passively regulated to target angles and are locked. Then, the manipulator with locked joints comes into use [13]. Because free-swinging joints can only be regulated passively, they are called as “passive joints,” and the healthy joints regulating passive joints are called “active joints.” The free-swinging joint failure treatment methods above either depend on motion planning or depend on the control method. No matter which method is used, it is significant to establish kinematic and dynamic models of underactuated manipulators and analyze kinematic and dynamic characteristics to make clear all coupling relationships inside the system at the beginning.

Kinematic and dynamic characteristic analysis has been extensively studied around underactuated manipulators on the ground. Aiming at a 2 DOF planar manipulator whose second joint is passive, Nakamura et al. [14] established its dynamic model based on the Hamiltonian function in phase space. Introducing periodic motion into an active joint, he drew Poincaré mapping figures to show the displacement relation between an active joint and a passive joint. Arai et al. [15] derived the unintegrable acceleration coupling relationship between active joints and a passive joint of a 3 DOF underactuated planar manipulator. The acceleration coupling relationship was called as “dynamic coupling relationship,” and it was the second-order nonholonomic constraint inside system. Lai et al. analyzed the dynamic coupling relationships of 2 DOF [16, 17], 3 DOF [18], 4 DOF [19], and  $n$  DOF [20] underactuated planar manipulators with the passive first joint and pointed out that when the first joint is passive, the second-order nonholonomic constraint could be integrated into the first-order nonholonomic constraint, so velocities of active joints and a passive joint were coupled. The researches above tell us that for underactuated planar manipulators, if only the first joint is passive, the underactuated system is with the first-order nonholonomic constraint, which represents that velocities of active joints and passive joints are coupled. Otherwise, the second-order nonholonomic constraint exists, and accelerations of active joints and passive joints are coupled.

The researches above used many geometric constraints of planar mechanism to simplify the analysis procedure, so they are only appropriate for underactuated planar manipulators. High DOF manipulators have three-dimensional geometric structure, so their kinematic and dynamic characteristic analysis is more complicated. Considering balance of gravity, English and Maciejewski [21] established the velocity mapping relation between joints and end-effector for  $n$  DOF underactuated manipulators. Bergerman and Xu [22] derived the second-order nonholonomic constraint which contained centrifugal force, Coriolis force, and gravitational torque and defined the local and global dynamic coupling indexes to depict acceleration transmission efficiency from active joints to passive joints, namely, dynamic coupling degree.

Analysis of high DOF underactuated manipulators on the ground must consider gravity effects. However, the space manipulator is free from gravity. Mukherjee and Chen [23] established a dynamic model of the space manipulator with free-swinging joints through the Lagrange equation and derived dynamic coupling relationship between active joints and passive joints based on the Hamiltonian operator. Aiming at the case that active joints are more than passive joints, He et al. [24] pointed out that “passive redundancy” existed when regulating passive joints. Then, they designed a sliding-mode controller with end-effector position/attitude correction, to minimize end-effector disturbance when regulating passive joints. Chen et al. [25] analyzed dynamic coupling relationship between an adjacent active joint and a passive joint for a space manipulator with single free-swinging joint failure and proposed a passive joint regulation strategy based on iteration control. The researches above treated the space manipulator base as fixed. In practice, space manipulators are installed on a free-floating base and motions between joints and the base are coupled. This coupled motion will act on kinematic and dynamic modeling. If it is neglected, we cannot establish valid kinematic and dynamic models and cannot reveal kinematic and dynamic coupling relationships of the space manipulator with free-swinging joint failure.

For the free-floating space manipulator, motion between the base and joints satisfies the first-order nonholonomic constraint originally because of momentum conservation without external force [26]. Moreover, according to existing researches about kinematic and dynamic modelling for underactuated manipulators, the second-order nonholonomic constraint also exists in accelerations among active joints, passive joints, and the base. Therefore, the free-floating space manipulator with free-swinging joint failure simultaneously contains the first-order nonholonomic constraint (kinematic coupling relationships) and the second-order nonholonomic constraint (dynamic coupling relationships), and they are independent. However, for underactuated manipulators on the ground, either the first-order nonholonomic constraint or the second-order nonholonomic constraint exists inside systems. Therefore, the kinematic and dynamic characteristic analysis of the free-floating space manipulator with free-swinging joint failure is more complicated than conventional underactuated manipulators, and all kinematic and dynamic coupling relationships need to be studied.

Aiming at the free-floating space manipulator with free-swinging joint failure, we establish the kinematic model based on the momentum conservation. Then, the partitioned dynamic equation corresponding to the distribution of active joints, passive joints, and the base are derived based on the Lagrange equation. Then, the kinematic and dynamic coupling relationships among active joints, passive joints, the base and end-effector are derived, and local and global coupling indexes are defined to evaluate the coupling degree. Finally, we briefly introduce motion planning and a control method for the space manipulator with free-swinging joint failure, as the reference of free-swinging joint failure treatment. The traits of this paper mainly include the following:

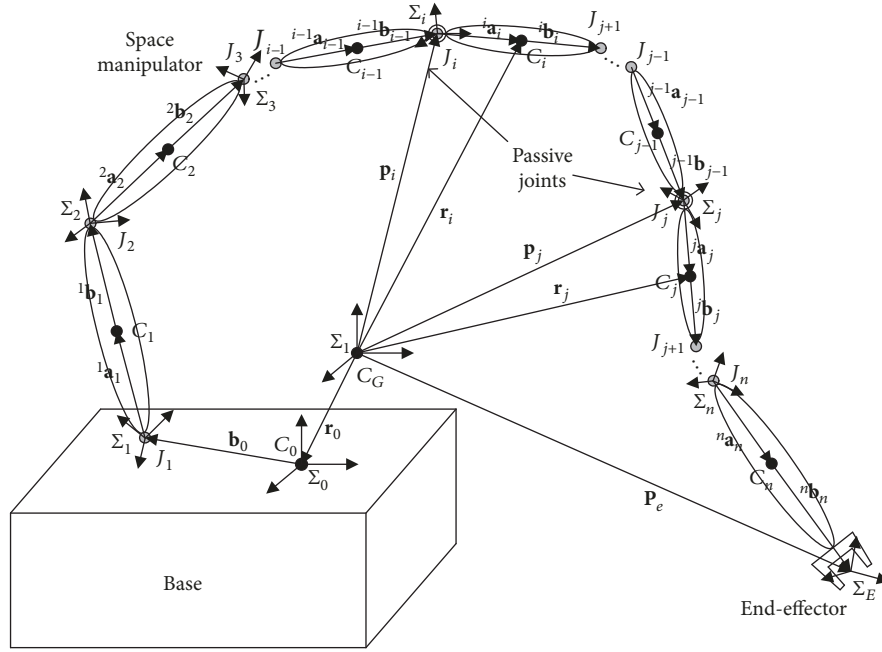


FIGURE 1: Kinematic model of the  $n$ -DOF space manipulator with free-swinging joint failure.

- (1) The general kinematic and dynamic modelling procedure of the free-floating space manipulator with free-swinging joint failure is proposed for the first time
- (2) We point out that the free-floating space manipulator with free-swinging joint failure simultaneously contains the first-order and second-order nonholonomic constraints, and we explicitly reveal all kinematic and dynamic coupling relationships among active joints, passive joints, free-floating base, and end-effector
- (3) We simply design motion planning and the control method based on the kinematic and dynamic coupling relationships for the free-floating space manipulator with free-swinging joint failure, and many tasks can be completed successfully

The remainder of this paper is as follows: Section II is the kinematic modelling of the free-floating space manipulator with free-swinging joint failure, and the velocity mapping relations between active joints, passive joints, base, and end-effector are derived. Then, we establish the partitioned dynamic model based on the Lagrange equation in Section III. In Section IV, all kinematic and dynamic coupling relationships inside the system are derived, and the local and global coupling indexes are defined. Then, motion planning and control methods for the free-floating space manipulator with free-swinging joint failure to execute tasks are designed. In Section V, simulation experiments are carried out to verify the existence and correctness of the first-order and second-order nonholonomic constraints and to display the execution effects of many tasks of the free-floating space manipulator with free-swinging joint failure. The conclusion is in Section VI.

## 2. Kinematic Modelling of the Free-Floating Space Manipulator with Free-Swinging Joint Failure

In this section, the kinematic model of the free-floating space manipulator with free-swinging joint failure is established and the expression of the conservation of system momentum is derived. Then, the velocity mapping relations between active joints, passive joints, the base, and end-effector are obtained.

*2.1. Kinematic Modelling.* An  $n$  DOF space manipulator with free-swinging joint failure is in Figure 1. In this paper, vectors and matrixes with subscript in the upper left corner are with respect to the corresponding coordinate frame and others with no subscript in the upper left corner are with respect to the inertial coordinate frame. Definitions of frequently used variables are as follow:

- $C_0$ : base centroid,
- $C_i$ : centroid of the  $i$ -th link,
- $C_G$ : centroid of the whole system,
- $J_i$ :  $i$ -th joint,  $i = 1, 2, \dots, n$ ,
- $\Sigma_i$ : inertial coordinate frame built at  $C_G$ ,
- $\Sigma_0$ : base coordinate frame built at  $C_0$ ,
- $\Sigma_i$ :  $i$ -th link coordinate frame built at  $C_i$ ,
- $\Sigma_E$ : end-effector coordinate frame,
- $m_0$ : base mass,
- $m_i$ : mass of the  $i$ -th link,
- $M$ : mass of the whole system,
- $\mathbf{I}_0 \in \mathbf{R}^{3 \times 3}$ : base inertia matrix with respect to  $C_0$ ,
- $\mathbf{I}_i \in \mathbf{R}^{3 \times 3}$ : inertia matrix of the  $i$ -th link with respect to  $C_i$ ,
- $\mathbf{p}_i \in \mathbf{R}^{3 \times 1}$ : position vector of  $J_i$ ,  $i = 1, 2, \dots, n$ ,

$\mathbf{p}_e = [x_e, y_e, z_e]^T \in \mathbf{R}^{3 \times 1}$ : position vector of end-effector,  
 $\Psi_e = [\alpha_e, \beta_e, \gamma_e]^T \in \mathbf{R}^{3 \times 1}$ : attitude vector of end-effector,  
 $\mathbf{r}_i \in \mathbf{R}^{3 \times 1}$ : position vector of  $C_i$ ,  $i = 1, 2, \dots, n$ ,  
 $\mathbf{r}_g \in \mathbf{R}^{3 \times 1}$ : position vector of  $C_G$  (if  $\sum_I$  is built at  $C_G$ ,  $\mathbf{r}_g \equiv \mathbf{0}$ ),  
 $\mathbf{r}_0 \in \mathbf{R}^{3 \times 1}$ : position vector of  $C_0$ ,  
 $\Psi_0 \in \mathbf{R}^{3 \times 1}$ : attitude vector of base,  
 $\mathbf{b}_0 \in \mathbf{R}^{3 \times 1}$ : position vector from  $C_0$  to  $J_1$ ,  
 $\theta = [\theta_1, \theta_2, \dots, \theta_n]^T \in \mathbf{R}^{n \times 1}$ : joint angle vector,  
 $\dot{\theta} = [\dot{\theta}_1, \dot{\theta}_2, \dots, \dot{\theta}_n]^T \in \mathbf{R}^{n \times 1}$ : joint velocity vector,  
 $\ddot{\theta} = [\ddot{\theta}_1, \ddot{\theta}_2, \dots, \ddot{\theta}_n]^T \in \mathbf{R}^{n \times 1}$ : joint acceleration vector,  
 $\mathbf{q} = [\mathbf{r}_0^T, \Psi_0^T, \theta^T]^T \in \mathbf{R}^{(n+6) \times 1}$ : state variable of system ( $\dot{\mathbf{q}}$  and  $\ddot{\mathbf{q}}$  are velocity and acceleration, respectively),  
 ${}^i\mathbf{R}_j \in \mathbf{R}^{3 \times 3}$ : attitude transformation matrix from  $\sum_j$  to  $\sum_i$ ,  
 ${}^i\mathbf{a}_i \in \mathbf{R}^{3 \times 1}$ : position vector from  $J_i$  to  $C_i$  ( $a_i$  is its norm,  $i = 1, 2, \dots, n$ ),  
 ${}^i\mathbf{b}_i \in \mathbf{R}^{3 \times 1}$ : position vector from  $C_i$  to  $J_{i+1}$  ( $b_i$  is its norm,  $i = 1, 2, \dots, n$ ),  
 $\mathbf{z}_i \in \mathbf{R}^{3 \times 1}$ : unit vector of the  $i$ -th joint axis,  $i = 1, 2, \dots, n$ ,  
 $\mathbf{v}_0, \omega_0 \in \mathbf{R}^{3 \times 1}$ : velocity of  $C_0$ /base angular velocity,  
 $\mathbf{v}_i, \omega_i \in \mathbf{R}^{3 \times 1}$ : velocity of  $C_i$ /angular velocity of the  $i$ -th link,  
 $\mathbf{v}_e, \omega_e \in \mathbf{R}^{3 \times 1}$ : end-effector velocity/end-effector angular velocity.

For a free-floating space manipulator, linear/angular velocities of  $i$ -th link and end-effector are

$$\begin{bmatrix} \mathbf{v}_i \\ \omega_i \end{bmatrix} = \begin{bmatrix} \mathbf{E}_3 & -\mathbf{r}_{0i}^\times \\ \mathbf{O}_3 & \mathbf{E}_3 \end{bmatrix} \begin{bmatrix} \mathbf{v}_0 \\ \omega_0 \end{bmatrix} + \begin{bmatrix} \mathbf{J}_{Li} \\ \mathbf{J}_{Ai} \end{bmatrix} \dot{\theta} = \mathbf{J}_{bi} \begin{bmatrix} \mathbf{v}_0 \\ \omega_0 \end{bmatrix} + \mathbf{J}_{mi} \dot{\theta}, \quad (1)$$

$$\begin{bmatrix} \mathbf{v}_e \\ \omega_e \end{bmatrix} = \begin{bmatrix} \mathbf{E}_3 & -\mathbf{p}_{0e}^\times \\ \mathbf{O}_3 & \mathbf{E}_3 \end{bmatrix} \begin{bmatrix} \mathbf{v}_0 \\ \omega_0 \end{bmatrix} + \begin{bmatrix} \mathbf{J}_{Le} \\ \mathbf{J}_{Ae} \end{bmatrix} \dot{\theta} = \mathbf{J}_b \begin{bmatrix} \mathbf{v}_0 \\ \omega_0 \end{bmatrix} + \mathbf{J}_m \dot{\theta}, \quad (2)$$

where  $\mathbf{J}_{Li} = [\mathbf{z}_1 \times (\mathbf{r}_i - \mathbf{p}_1), \mathbf{z}_2 \times (\mathbf{r}_i - \mathbf{p}_2), \dots, \mathbf{z}_i \times (\mathbf{r}_i - \mathbf{p}_i), \mathbf{0}, \dots, \mathbf{0}] \in \mathbf{R}^{3 \times n}$ ,  $\mathbf{J}_{Le} = [\mathbf{z}_1 \times (\mathbf{p}_e - \mathbf{p}_1), \mathbf{z}_2 \times (\mathbf{p}_e - \mathbf{p}_2), \dots, \mathbf{z}_n \times (\mathbf{p}_e - \mathbf{p}_n)] \in \mathbf{R}^{3 \times n}$ ,  $\mathbf{J}_{Ai} = [\mathbf{z}_1, \mathbf{z}_2, \dots, \mathbf{z}_i, \mathbf{0}, \dots, \mathbf{0}] \in \mathbf{R}^{3 \times n}$ , and  $\mathbf{J}_{Ae} = [\mathbf{z}_1, \mathbf{z}_2, \dots, \mathbf{z}_i, \dots, \mathbf{z}_n] \in \mathbf{R}^{3 \times n}$  and where  $\mathbf{p}_{0e} = \mathbf{p}_e - \mathbf{r}_0$  and  $\mathbf{r}_{0i} = \mathbf{r}_i - \mathbf{r}_0$  and  $\mathbf{p}_{0e}^\times$  and  $\mathbf{r}_{0i}^\times$  are the antisymmetric matrixes of  $\mathbf{p}_{0e}$  and  $\mathbf{r}_{0i}$ , respectively.  $\mathbf{E}_3 \in \mathbf{R}^{3 \times 3}$  is a unit matrix, and  $\mathbf{O}_3 \in \mathbf{R}^{3 \times 3}$  is a zero matrix.  $\mathbf{J}_b \in \mathbf{R}^{6 \times 6}$  denotes base Jacobian matrixes representing the transmission from  $[\mathbf{v}_0^T, \omega_0^T]^T$  to  $[\mathbf{v}_i^T, \omega_i^T]^T$ ,  $[\mathbf{v}_e^T, \omega_e^T]^T$ .  $\mathbf{J}_{mi} \in \mathbf{R}^{6 \times n}$  and  $\mathbf{J}_m \in \mathbf{R}^{6 \times n}$  denote manipulator Jacobian matrixes representing the transmission from  $\dot{\theta}$  to  $[\mathbf{v}_i^T, \omega_i^T]^T$ ,  $[\mathbf{v}_e^T, \omega_e^T]^T$ .

$\mathbf{J}_m$  consists of  $n$  column vectors:  $\mathbf{J}_m = [\mathbf{j}_{m1}, \mathbf{j}_{m2}, \dots, \mathbf{j}_{mn}] \in \mathbf{R}^{6 \times n}$ . So  $\mathbf{J}_m \dot{\theta}$  can be expressed as

$$\mathbf{J}_m \dot{\theta} = \sum_{i=1}^n \mathbf{j}_{mi} \dot{\theta}_i. \quad (3)$$

As can be seen from equation (3),  $\mathbf{j}_{mi}$  depicts the contribution of  $i$ -th joint velocity  $\dot{\theta}_i$  to  $[\mathbf{v}_e^T, \omega_e^T]^T$ . If selecting

the rest of the healthy joints as active joints, we can obtain a serial number set of passive joints as  $S_p = \{s_{pi} | \forall s_{pi} \in \{1, 2, \dots, n\}, i = 1, 2, \dots, p\}$  and serial number set of active joints as  $S_a = \{s_{Aj} | \forall s_{Aj} \in \{1, 2, \dots, n\}, j = 1, 2, \dots, a\}$ . So the passive joint velocity is  $\dot{\theta}_p = [\dot{\theta}_{p1}, \dot{\theta}_{p2}, \dots, \dot{\theta}_{pp}]^T = [\dot{\theta}_{s_{p1}}, \dot{\theta}_{s_{p2}}, \dots, \dot{\theta}_{s_{pp}}]^T$ , and the active joint velocity is  $\dot{\theta}_a = [\dot{\theta}_{a1}, \dot{\theta}_{a2}, \dots, \dot{\theta}_{aa}]^T = [\dot{\theta}_{s_{a1}}, \dot{\theta}_{s_{a2}}, \dots, \dot{\theta}_{s_{aa}}]^T$ . With the help of the commutative law of addition, we express equation (3) as

$$\begin{aligned} \mathbf{J}_m \dot{\theta} &= \sum_{j=1}^p \mathbf{j}_{ms_{pj}} \dot{\theta}_{pj} + \sum_{k=1}^a \mathbf{j}_{ms_{ak}} \dot{\theta}_{ak} \\ &= \mathbf{J}_{mp} \dot{\theta}_p + \mathbf{J}_{ma} \dot{\theta}_a = [\mathbf{J}_{mp} \ \mathbf{J}_{ma}] \begin{bmatrix} \dot{\theta}_p \\ \dot{\theta}_a \end{bmatrix}, \end{aligned} \quad (4)$$

where  $\mathbf{j}_{ms_{pj}}$ ,  $j = 1, 2, \dots, p$ , is the column vectors corresponding to passive joints, and they make up  $\mathbf{J}_{mp} \in \mathbf{R}^{6 \times p}$  which represents transmission from  $\dot{\theta}_p$  to  $[\mathbf{v}_e^T, \omega_e^T]^T$ .  $\mathbf{j}_{ms_{ak}}$ ,  $k = 1, 2, \dots, a$ , is the column vectors corresponding to active joints, and they make up  $\mathbf{J}_{ma} \in \mathbf{R}^{6 \times a}$  which represents transmission from  $\dot{\theta}_a$  to  $[\mathbf{v}_e^T, \omega_e^T]^T$ . If making  $\dot{\theta}_b = [\mathbf{v}_0^T, \omega_0^T]^T \in \mathbf{R}^{6 \times 1}$ , equation (2) becomes

$$\begin{bmatrix} \mathbf{v}_e \\ \omega_e \end{bmatrix} = \mathbf{J}_b \dot{\theta}_b + \mathbf{J}_{mp} \dot{\theta}_p + \mathbf{J}_{ma} \dot{\theta}_a = [\mathbf{J}_b \ \mathbf{J}_{mp} \ \mathbf{J}_{ma}] \begin{bmatrix} \dot{\theta}_b \\ \dot{\theta}_p \\ \dot{\theta}_a \end{bmatrix}. \quad (5)$$

If we know the desired  $[\mathbf{v}_e^T, \omega_e^T]^T$ , we can acquire  $\dot{\theta}_b$ ,  $\dot{\theta}_p$ , and  $\dot{\theta}_a$  from equation (5). However, the base and passive joints cannot actively supply  $\dot{\theta}_b$  and  $\dot{\theta}_p$  because of lacking actuators. All motions of passive joints, base, and end-effector can only be actuated by active joints. In the next subsection, we are going to derive specific velocity mapping relations among active joints, passive joints, base, and end-effector based on conservation of system momentum.

**2.2. Velocity Mapping Relations between Active Joints, Passive Joints, Base, and End-Effector Based on Momentum Conservation.** Linear momentum and angular momentum of the whole system are

$$\mathbf{P} = \sum_{i=0}^n m_i \mathbf{v}_i = M \mathbf{v}_0 - M \mathbf{r}_0^\times \omega_0 + \mathbf{J}_{LM} \dot{\theta}, \quad (6)$$

$$\begin{aligned} \mathbf{L} &= \sum_{i=0}^n (\mathbf{I}_i \omega_i + m_i \mathbf{r}_i \times \mathbf{v}_i) \\ &= \left[ \mathbf{I}_0 + \sum_{i=1}^n (\mathbf{I}_i - m_i \mathbf{r}_i \times \mathbf{r}_{0i}^\times) \right] \omega_0 + \mathbf{J}_{AM} \dot{\theta}, \end{aligned} \quad (7)$$

where  $\mathbf{J}_{LM} = \sum_{i=1}^n m_i \mathbf{J}_{Li} \in \mathbf{R}^{3 \times n}$  represents the contribution of  $\dot{\theta}$  to linear momentum  $\mathbf{P}$  and  $\mathbf{J}_{AM} = \sum_{i=1}^n (\mathbf{I}_i \mathbf{J}_{Ai} + m_i \mathbf{r}_i^\times \mathbf{J}_{Li}) \in \mathbf{R}^{3 \times n}$  represents the contribution of  $\dot{\theta}$  to angular momentum  $\mathbf{L}$ .  $\mathbf{J}_{LM}$  and  $\mathbf{J}_{AM}$  can be expressed as  $\mathbf{J}_{LM} = [\mathbf{j}_{LM1}, \mathbf{j}_{LM2}, \dots, \mathbf{j}_{LMn}]$  and  $\mathbf{J}_{AM} = [\mathbf{j}_{AM1}, \mathbf{j}_{AM2}, \dots, \mathbf{j}_{AMn}]$ , respectively, and we can find column vectors corresponding to passive joints and active joints to make up matrixes

$$\begin{aligned} \mathbf{J}_{LMA} &= [\mathbf{j}_{LMS_{A1}}, \mathbf{j}_{LMS_{A2}}, \dots, \mathbf{j}_{LMS_{Aa}}] \in \mathbf{R}^{3 \times a}, \\ \mathbf{J}_{AMA} &= [\mathbf{j}_{AMS_{A1}}, \mathbf{j}_{AMS_{A2}}, \dots, \mathbf{j}_{AMS_{Aa}}] \in \mathbf{R}^{3 \times a}, \\ \mathbf{J}_{LMP} &= [\mathbf{j}_{LMS_{p1}}, \mathbf{j}_{LMS_{p2}}, \dots, \mathbf{j}_{LMS_{pp}}] \in \mathbf{R}^{3 \times p}, \\ \mathbf{J}_{AMP} &= [\mathbf{j}_{AMS_{p1}}, \mathbf{j}_{AMS_{p2}}, \dots, \mathbf{j}_{AMS_{pp}}] \in \mathbf{R}^{3 \times p}. \end{aligned} \quad (8)$$

Equations (6) and (7) can be expressed in matrix form

$$\begin{bmatrix} \mathbf{P} \\ \mathbf{L} \end{bmatrix} = \begin{bmatrix} M\mathbf{E}_3 & -M\mathbf{r}_0^\times \\ \mathbf{O}_3 & \mathbf{I}_\omega \end{bmatrix} \begin{bmatrix} \mathbf{v}_0 \\ \omega_0 \end{bmatrix} + \begin{bmatrix} \mathbf{J}_{LMA} \\ \mathbf{J}_{AMA} \end{bmatrix} \dot{\theta}_A + \begin{bmatrix} \mathbf{J}_{LMP} \\ \mathbf{J}_{AMP} \end{bmatrix} \dot{\theta}_P, \quad (9)$$

where  $\mathbf{I}_\omega = \mathbf{I}_0 + \sum_{i=1}^n (\mathbf{I}_i - m_i \mathbf{r}_i^\times \mathbf{r}_{0i}^\times) \in \mathbf{R}^{3 \times 3}$ . Without the external force, system momentum is conservative. Setting the initial momentum is zero, so

$$\begin{bmatrix} M\mathbf{E}_3 & -M\mathbf{r}_0^\times \\ \mathbf{O}_3 & \mathbf{I}_\omega \end{bmatrix} \begin{bmatrix} \mathbf{v}_0 \\ \omega_0 \end{bmatrix} + \begin{bmatrix} \mathbf{J}_{TMLA} \\ \mathbf{J}_{AIAA} \end{bmatrix} \dot{\theta}_A + \begin{bmatrix} \mathbf{J}_{TMLP} \\ \mathbf{J}_{AIAP} \end{bmatrix} \dot{\theta}_P = \begin{bmatrix} 0 \\ 0 \end{bmatrix}. \quad (10)$$

From equation (10), we know that  $\dot{\theta}_A$ ,  $\dot{\theta}_P$ , and  $\dot{\theta}_b$  are coupled with each other, but we care more about the transmission from  $\dot{\theta}_A$  to  $\dot{\theta}_P$  and  $\dot{\theta}_b$ . From equation (10), we have

$$\begin{bmatrix} \mathbf{J}_{TMLA} \\ \mathbf{J}_{AIAA} \end{bmatrix} \dot{\theta}_A + \begin{bmatrix} M\mathbf{E}_3 & -M\mathbf{r}_0^\times & \mathbf{J}_{TMLP} \\ \mathbf{O}_3 & \mathbf{I}_\omega & \mathbf{J}_{AIAP} \end{bmatrix} \begin{bmatrix} \dot{\theta}_b \\ \dot{\theta}_P \end{bmatrix} = \begin{bmatrix} 0 \\ 0 \end{bmatrix}. \quad (11)$$

Making

$$\begin{aligned} \mathbf{H}_A &= \begin{bmatrix} \mathbf{J}_{TMLA} \\ \mathbf{J}_{AIAA} \end{bmatrix} \in \mathbf{R}^{6 \times a}, \\ \mathbf{H}_{bP} &= \begin{bmatrix} M\mathbf{E}_3 & -M\mathbf{r}_0^\times & \mathbf{J}_{TMLP} \\ \mathbf{O}_3 & \mathbf{I}_\omega & \mathbf{J}_{AIAP} \end{bmatrix} \in \mathbf{R}^{6 \times (p+6)}, \end{aligned} \quad (12)$$

Equation (11) becomes

$$\mathbf{H}_A \dot{\theta}_A + \mathbf{H}_{bP} \begin{bmatrix} \dot{\theta}_b \\ \dot{\theta}_P \end{bmatrix} = \begin{bmatrix} 0 \\ 0 \end{bmatrix}. \quad (13)$$

Then, we can obtain transmission from  $\dot{\theta}_A$  to  $\dot{\theta}_P$  and  $\dot{\theta}_b$ :

$$\begin{bmatrix} \dot{\theta}_b \\ \dot{\theta}_P \end{bmatrix} = \mathbf{J}_{bPA} \dot{\theta}_A + (\mathbf{E}_{6+p} - \mathbf{H}_{bP}^+ \mathbf{H}_{bP}) \xi. \quad (14)$$

$\mathbf{J}_{bPA} = -\mathbf{H}_{bP}^+ \mathbf{H}_A \in \mathbf{R}^{(6+p) \times a}$  represents the Jacobian matrix from  $\dot{\theta}_A$  to  $\dot{\theta}_P$  and  $\dot{\theta}_b$ .  $(\mathbf{E}_{6+p} - \mathbf{H}_{bP}^+ \mathbf{H}_{bP}) \xi$  is the null space of  $\mathbf{H}_{bP}$ , and  $\xi$  is an arbitrary vector. Because  $6 < 6 + p$ , when  $\mathbf{H}_{bP}$  is full rank, the null space exists. In particular, making  $\xi = 0$ , we can obtain transmission from  $\dot{\theta}_A$  to  $\dot{\theta}_P$  and from  $\dot{\theta}_A$  to  $\dot{\theta}_b$ :

$$\begin{aligned} \dot{\theta}_b &= \mathbf{J}_{bA} \dot{\theta}_A, \\ \dot{\theta}_P &= \mathbf{J}_{PA} \dot{\theta}_A. \end{aligned} \quad (15)$$

$\mathbf{J}_{bA} \in \mathbf{R}^{6 \times a}$  is the first six rows of vectors of  $\mathbf{J}_{bPA}$ , and  $\mathbf{J}_{PA} \in \mathbf{R}^{p \times a}$  is the last  $p$  rows of vectors of  $\mathbf{J}_{bPA}$ . Substituting equation (15) into equation (5), we obtain the transmission from  $\dot{\theta}_A$  to  $[\mathbf{v}_e^T, \omega_e^T]^T$ :

$$\begin{bmatrix} \mathbf{v}_e \\ \omega_e \end{bmatrix} = (\mathbf{J}_{bP} \mathbf{J}_{bPA} + \mathbf{J}_{mA}) \dot{\theta}_A = \mathbf{J}_{eA} \dot{\theta}_A, \quad (16)$$

where  $\mathbf{J}_{bP} = [\mathbf{J}_b \quad \mathbf{J}_{mP}] \in \mathbf{R}^{6 \times (p+6)}$ , and  $\mathbf{J}_{eA} = \mathbf{J}_{bP} \mathbf{J}_{bPA} + \mathbf{J}_{mA} \in \mathbf{R}^{6 \times a}$  is the Jacobian matrix representing transmission from  $\dot{\theta}_A$  to  $[\mathbf{v}_e^T, \omega_e^T]^T$ . Equations (15) and (16) can be reduced to the following constraints:

$$\begin{aligned} \mathbf{h}_1(\dot{\theta}_P, \dot{\theta}_A, t) &= 0, \\ \mathbf{h}_2(\dot{\theta}_b, \dot{\theta}_A, t) &= 0, \\ \mathbf{h}_3(\mathbf{v}_e, \omega_e, \dot{\theta}_A, t) &= 0. \end{aligned} \quad (17)$$

Obviously, for space manipulators, there is no definite relation between  $\theta_A$  and  $\theta_P, \theta_b, p_e, \Psi_e$ , which means we cannot find constraints like  $\mathbf{h}_{10}(\theta_P, \theta_A, t) = 0$ ,  $\mathbf{h}_{20}(\theta_b, \theta_A, t) = 0$ , and  $\mathbf{h}_{30}(\mathbf{p}_e, \Psi_e, \theta_A, t) = 0$  making  $\mathbf{h}_1 = d\mathbf{h}_{10}/dt$ ,  $\mathbf{h}_2 = d\mathbf{h}_{20}/dt$ , and  $\mathbf{h}_3 = d\mathbf{h}_{30}/dt$ , so constraints in equation (17) are nonholonomic. Because equation (17) includes constraints among the first-order derivatives of  $\theta_b, \theta_A, \theta_P, \mathbf{p}_e, \Psi_e$ , it is called as the first-order nonholonomic constraint. The first-order nonholonomic constraint is unique for the free-floating space manipulator with free-swinging joint failure because its momentum is conservative.

### 3. Dynamic Modelling of the Free-Floating Space Manipulator with Free-Swinging Joint Failure

Establishment of a dynamic model is the basis of dynamic coupling relationship analysis and controller design, so the

dynamic model of the space manipulator with free-swinging joint failure is established in this section.

**3.1. Kinetic Energy of System.** The Lagrange function of the space manipulator with free-swinging joint failure is as follows:

$$L = K - E, \quad (18)$$

where  $K$  is system kinetic energy and  $E$  is the system potential energy. The space manipulator is free from gravity, and we take no account of joint and link flexibility, so  $E = 0$ . The Lagrange function equals to total kinetic energy:

$$\begin{aligned} L &= K = \sum_{i=0}^n \left( \frac{1}{2} m_i \mathbf{v}_i^T \mathbf{v}_i + \frac{1}{2} \omega_i^T \mathbf{I}_i \omega_i \right) \\ &= \frac{1}{2} \begin{bmatrix} \dot{\theta}_b^T & \dot{\theta}^T \end{bmatrix} \begin{bmatrix} \mathbf{M}_b & \mathbf{M}_{bm} \\ \mathbf{M}_{mb} & \mathbf{M}_m \end{bmatrix} \begin{bmatrix} \dot{\theta}_b \\ \dot{\theta} \end{bmatrix} \\ &= \frac{1}{2} \begin{bmatrix} \dot{\theta}_b^T & \dot{\theta}^T \end{bmatrix} \mathbf{M} \begin{bmatrix} \dot{\theta}_b \\ \dot{\theta} \end{bmatrix}, \end{aligned} \quad (19)$$

where

$$\begin{aligned} \mathbf{M}_b &= \begin{bmatrix} M\mathbf{E}_3 & -M\mathbf{r}_0^\times \\ -M\mathbf{r}_0^{\times T} & \sum_{i=0}^n (m_i \mathbf{r}_{0i}^{\times T} \mathbf{r}_{0i}^\times + \mathbf{I}_i) \end{bmatrix} \in \mathbf{R}^{6 \times 6}, \\ \mathbf{M}_{bm} &= \begin{bmatrix} \sum_{i=0}^n m_i \mathbf{J}_{Li} \\ \sum_{i=0}^n (-m_i \mathbf{r}_{0i}^{\times T} \mathbf{J}_{Li} + \mathbf{I}_i \mathbf{J}_{Ai}) \end{bmatrix} \in \mathbf{R}^{6 \times n}, \\ \mathbf{M}_{mb} &= \mathbf{M}_{bm}^T = \begin{bmatrix} \sum_{i=0}^n m_i \mathbf{J}_{Li}^T & \sum_{i=0}^n (-m_i \mathbf{J}_{Li}^T \mathbf{r}_{0i}^\times + \mathbf{J}_{Ai}^T \mathbf{I}_i) \end{bmatrix} \in \mathbf{R}^{n \times 6}, \\ \mathbf{M}_m &= \sum_{i=0}^n (m_i \mathbf{J}_{Li}^T \mathbf{J}_{Li} + \mathbf{J}_{Ai}^T \mathbf{I}_i \mathbf{J}_{Ai}) \in \mathbf{R}^{n \times n}, \\ \mathbf{M} &= \begin{bmatrix} \mathbf{M}_b & \mathbf{M}_{bm} \\ \mathbf{M}_{mb} & \mathbf{M}_m \end{bmatrix} \in \mathbf{R}^{(n+6) \times (n+6)}. \end{aligned} \quad (20)$$

$\mathbf{M}_b$  denotes the base inertia matrix.  $\mathbf{M}_m$  denotes the manipulator inertia matrix.  $\mathbf{M}_{bm}$  and  $\mathbf{M}_{mb}$  are the coupling inertia matrixes between base and manipulator.  $\mathbf{M}$  is the inertia matrix of the whole system. Expanding equation (19), we have

$$L = \frac{1}{2} \left( \dot{\theta}_b^T \mathbf{M}_b \dot{\theta}_b + \dot{\theta}^T \mathbf{M}_{mb} \dot{\theta}_b + \dot{\theta}_b^T \mathbf{M}_{bm} \dot{\theta} + \dot{\theta}^T \mathbf{M}_m \dot{\theta} \right). \quad (21)$$

We can know that  $\mathbf{M}_{bm}$ ,  $\mathbf{M}_{mb}$ , and  $\mathbf{M}_m$  are relative to joint velocity, so we can utilize commutative law of addition

to divide these matrixes into

$$\begin{aligned} \dot{\theta}^T \mathbf{M}_{mb} &= \dot{\theta}_1 \mathbf{m}_{mb\_row1} + \dot{\theta}_2 \mathbf{m}_{mb\_row2} + \cdots + \dot{\theta}_n \mathbf{m}_{mb\_rown}, \\ \mathbf{M}_{bm} \dot{\theta} &= \mathbf{m}_{bm\_col1} \dot{\theta}_1 + \mathbf{m}_{bm\_col2} \dot{\theta}_2 + \cdots + \mathbf{m}_{bm\_coln} \dot{\theta}_n, \\ \dot{\theta}^T \mathbf{M}_m \dot{\theta} &= \sum_{i=1}^n \sum_{j=1}^n \dot{\theta}_i m_{mij} \dot{\theta}_j. \end{aligned} \quad (22)$$

The row vector  $\mathbf{m}_{mb\_rowi}$  of  $\mathbf{M}_{mb}$ , the column vector  $\mathbf{m}_{bm\_coli}$  of  $\mathbf{M}_{bm}$ , and the element  $m_{mij}$  of  $\mathbf{M}_m$  represent the contribution of the corresponding joint velocity to kinetic energy. Then, equation (21) can be expressed as

$$\begin{aligned} L &= \frac{1}{2} \left( \dot{\theta}_b^T \mathbf{M}_b \dot{\theta}_b + \begin{bmatrix} \dot{\theta}_P^T & \dot{\theta}_A^T \end{bmatrix} \begin{bmatrix} \mathbf{M}_{mbP} \\ \mathbf{M}_{mbA} \end{bmatrix} \dot{\theta}_b \right. \\ &\quad + \dot{\theta}_b^T \begin{bmatrix} \mathbf{M}_{bmP} & \mathbf{M}_{bmA} \end{bmatrix} \begin{bmatrix} \dot{\theta}_P \\ \dot{\theta}_A \end{bmatrix} \\ &\quad \left. + \begin{bmatrix} \dot{\theta}_P^T & \dot{\theta}_A^T \end{bmatrix} \begin{bmatrix} \mathbf{M}_{mPP} & \mathbf{M}_{mPA} \\ \mathbf{M}_{mAP} & \mathbf{M}_{mAA} \end{bmatrix} \begin{bmatrix} \dot{\theta}_P \\ \dot{\theta}_A \end{bmatrix} \right), \end{aligned} \quad (23)$$

where

$$\begin{aligned} \mathbf{M}_{mbP} &= \begin{bmatrix} \mathbf{m}_{mb\_rowSp1} \\ \mathbf{m}_{mb\_rowSp2} \\ \vdots \\ \mathbf{m}_{mb\_rowSpP} \end{bmatrix} \in \mathbf{R}^{P \times 6}, \\ \mathbf{M}_{mbA} &= \begin{bmatrix} \mathbf{m}_{mb\_rowSA1} \\ \mathbf{m}_{mb\_rowSA2} \\ \vdots \\ \mathbf{m}_{mb\_rowSAa} \end{bmatrix} \in \mathbf{R}^{a \times 6}, \\ \mathbf{M}_{bmP} &= \begin{bmatrix} \mathbf{m}_{bm\_colSp1} & \mathbf{m}_{bm\_colSp2} & \cdots & \mathbf{m}_{bm\_colSpP} \end{bmatrix} \in \mathbf{R}^{6 \times P}, \\ \mathbf{M}_{bmA} &= \begin{bmatrix} \mathbf{m}_{bm\_colSA1} & \mathbf{m}_{bm\_colSA2} & \cdots & \mathbf{m}_{bm\_colSAa} \end{bmatrix} \in \mathbf{R}^{6 \times a}, \\ \mathbf{M}_{mPP} &= \begin{bmatrix} m_{mS_{p1}S_{p1}} & m_{mS_{p1}S_{p2}} & \cdots & m_{mS_{p1}S_{pP}} \\ m_{mS_{p2}S_{p1}} & m_{mS_{p2}S_{p2}} & \cdots & m_{mS_{p2}S_{pP}} \\ \vdots & \vdots & \ddots & \vdots \\ m_{mS_{pP}S_{p1}} & m_{mS_{pP}S_{p2}} & \cdots & m_{mS_{pP}S_{pP}} \end{bmatrix} \in \mathbf{R}^{P \times P}, \\ \mathbf{M}_{mAA} &= \begin{bmatrix} m_{mS_{A1}S_{A1}} & m_{mS_{A1}S_{A2}} & \cdots & m_{mS_{A1}S_{Aa}} \\ m_{mS_{A2}S_{A1}} & m_{mS_{A2}S_{A2}} & \cdots & m_{mS_{A2}S_{Aa}} \\ \vdots & \vdots & \ddots & \vdots \\ m_{mS_{Aa}S_{A1}} & m_{mS_{Aa}S_{A2}} & \cdots & m_{mS_{Aa}S_{Aa}} \end{bmatrix} \in \mathbf{R}^{a \times a}, \end{aligned}$$

$$\mathbf{M}_{mAP} = \begin{bmatrix} m_{mS_{A1}S_{P1}} & m_{mS_{A1}S_{P2}} & \cdots & m_{mS_{A1}S_{Pp}} \\ m_{mS_{A2}S_{P1}} & m_{mS_{A2}S_{P2}} & \cdots & m_{mS_{A2}S_{Pp}} \\ \vdots & \vdots & \ddots & \vdots \\ m_{mS_{Aa}S_{P1}} & m_{mS_{Aa}S_{P2}} & \cdots & m_{mS_{Aa}S_{Pp}} \end{bmatrix} \in \mathbf{R}^{a \times p},$$

$$\mathbf{M}_{mPA} = \begin{bmatrix} m_{mS_{P1}S_{A1}} & m_{mS_{P1}S_{A2}} & \cdots & m_{mS_{P1}S_{Aa}} \\ m_{mS_{P2}S_{A1}} & m_{mS_{P2}S_{A2}} & \cdots & m_{mS_{P2}S_{Aa}} \\ \vdots & \vdots & \ddots & \vdots \\ m_{mS_{Pp}S_{A1}} & m_{mS_{Pp}S_{A2}} & \cdots & m_{mS_{Pp}S_{Aa}} \end{bmatrix} \in \mathbf{R}^{p \times a}.$$

$\mathbf{M}$  becomes

$$\mathbf{M} = \begin{bmatrix} \mathbf{M}_b & \mathbf{M}_{bmP} & \mathbf{M}_{bmA} \\ \mathbf{M}_{mbP} & \mathbf{M}_{mPP} & \mathbf{M}_{mPA} \\ \mathbf{M}_{mbA} & \mathbf{M}_{mAP} & \mathbf{M}_{mAA} \end{bmatrix}. \quad (25)$$

And the Lagrange function of the system is

$$L = \frac{1}{2} \begin{bmatrix} \dot{\theta}_b^T & \dot{\theta}_P^T & \dot{\theta}_A^T \end{bmatrix} \begin{bmatrix} \mathbf{M}_b & \mathbf{M}_{bmP} & \mathbf{M}_{bmA} \\ \mathbf{M}_{mbP} & \mathbf{M}_{mPP} & \mathbf{M}_{mPA} \\ \mathbf{M}_{mbA} & \mathbf{M}_{mAP} & \mathbf{M}_{mAA} \end{bmatrix} \begin{bmatrix} \dot{\theta}_b \\ \dot{\theta}_P \\ \dot{\theta}_A \end{bmatrix}$$

$$= \frac{1}{2} \left( \dot{\theta}_b^T \mathbf{M}_b \dot{\theta}_b + \dot{\theta}_P^T \mathbf{M}_{mbP} \dot{\theta}_b + \dot{\theta}_A^T \mathbf{M}_{mbA} \dot{\theta}_b + \dot{\theta}_b^T \mathbf{M}_{bmP} \dot{\theta}_P \right.$$

$$+ \dot{\theta}_P^T \mathbf{M}_{mPP} \dot{\theta}_P + \dot{\theta}_A^T \mathbf{M}_{mAP} \dot{\theta}_P + \dot{\theta}_b^T \mathbf{M}_{bmA} \dot{\theta}_A$$

$$\left. + \dot{\theta}_P^T \mathbf{M}_{mPA} \dot{\theta}_A + \dot{\theta}_A^T \mathbf{M}_{mAA} \dot{\theta}_A \right). \quad (26)$$

3.2. Lagrange Equation of the System. The Lagrange equation is

$$\begin{cases} \frac{d}{dt} \left( \frac{\partial L}{\partial \dot{\theta}_b} \right) - \frac{\partial L}{\partial \theta_b} = \tau_b, \\ \frac{d}{dt} \left( \frac{\partial L}{\partial \dot{\theta}_P} \right) - \frac{\partial L}{\partial \theta_P} = \tau_P, \\ \frac{d}{dt} \left( \frac{\partial L}{\partial \dot{\theta}_A} \right) - \frac{\partial L}{\partial \theta_A} = \tau_A. \end{cases} \quad (27)$$

Substituting equation (26) into equation (27), and calculating derivatives, we have

$$\begin{cases} \frac{d}{dt} \left( \frac{\partial L}{\partial \dot{\theta}_b} \right) = \mathbf{M}_b \ddot{\theta}_b + \mathbf{M}_{bmP} \ddot{\theta}_P + \mathbf{M}_{bmA} \ddot{\theta}_A + \sum_{i=1}^{6+n} \frac{\partial \mathbf{M}_b}{\partial q_i} \dot{q}_i \cdot \dot{\theta}_b + \sum_{i=1}^{6+n} \frac{\partial \mathbf{M}_{bmP}}{\partial q_i} \dot{q}_i \cdot \dot{\theta}_P + \sum_{i=1}^{6+n} \frac{\partial \mathbf{M}_{bmA}}{\partial q_i} \dot{q}_i \cdot \dot{\theta}_A, \\ \frac{d}{dt} \left( \frac{\partial L}{\partial \dot{\theta}_P} \right) = \mathbf{M}_{mbP} \ddot{\theta}_b + \mathbf{M}_{mPP} \ddot{\theta}_P + \mathbf{M}_{mPA} \ddot{\theta}_A + \sum_{i=1}^{6+n} \frac{\partial \mathbf{M}_{mbP}}{\partial q_i} \dot{q}_i \cdot \dot{\theta}_b + \sum_{i=1}^{6+n} \frac{\partial \mathbf{M}_{mPP}}{\partial q_i} \dot{q}_i \cdot \dot{\theta}_P + \sum_{i=1}^{6+n} \frac{\partial \mathbf{M}_{mPA}}{\partial q_i} \dot{q}_i \cdot \dot{\theta}_A, \\ \frac{d}{dt} \left( \frac{\partial L}{\partial \dot{\theta}_A} \right) = \mathbf{M}_{mbA} \ddot{\theta}_b + \mathbf{M}_{mAP} \ddot{\theta}_P + \mathbf{M}_{mAA} \ddot{\theta}_A + \sum_{i=1}^{6+n} \frac{\partial \mathbf{M}_{mbA}}{\partial q_i} \dot{q}_i \cdot \dot{\theta}_b + \sum_{i=1}^{6+n} \frac{\partial \mathbf{M}_{mAP}}{\partial q_i} \dot{q}_i \cdot \dot{\theta}_P + \sum_{i=1}^{6+n} \frac{\partial \mathbf{M}_{mAA}}{\partial q_i} \dot{q}_i \cdot \dot{\theta}_A. \end{cases} \quad (28)$$

Making  $\mathbf{c}_{\tau_{b-1}} = \sum_{i=1}^{6+n} (\partial \mathbf{M}_b / \partial q_i) \dot{q}_i \cdot \dot{\theta}_b + \sum_{i=1}^{6+n} (\partial \mathbf{M}_{bmP} / \partial q_i) \dot{q}_i \cdot \dot{\theta}_P + \sum_{i=1}^{6+n} (\partial \mathbf{M}_{bmA} / \partial q_i) \dot{q}_i \cdot \dot{\theta}_A$ ,  $\mathbf{c}_{\tau_{p-1}} = \sum_{i=1}^{6+n} (\partial \mathbf{M}_{mbP} / \partial q_i) \dot{q}_i \cdot \dot{\theta}_b + \sum_{i=1}^{6+n} (\partial \mathbf{M}_{mPP} / \partial q_i) \dot{q}_i \cdot \dot{\theta}_P + \sum_{i=1}^{6+n} (\partial \mathbf{M}_{mPA} / \partial q_i) \dot{q}_i \cdot \dot{\theta}_A$ , and  $\mathbf{c}_{\tau_{a-1}} = \sum_{i=1}^{6+n} (\partial \mathbf{M}_{mbA} / \partial q_i) \dot{q}_i \cdot \dot{\theta}_b + \sum_{i=1}^{6+n} (\partial \mathbf{M}_{mAP} / \partial q_i) \dot{q}_i \cdot \dot{\theta}_P + \sum_{i=1}^{6+n} (\partial \mathbf{M}_{mAA} / \partial q_i) \dot{q}_i \cdot \dot{\theta}_A$ . And  $\mathbf{c}_{\tau_{b-2}} = \partial L / \partial \theta_b$ ,  $\mathbf{c}_{\tau_{p-2}} = \partial L / \partial \theta_P$ , and  $\mathbf{c}_{\tau_{a-2}} = \partial L / \partial \theta_A$ .

$\mathbf{c}_{\tau_{b-1}}, \mathbf{c}_{\tau_{p-2}} \in \mathbf{R}^{6 \times 1}$ ,  $\mathbf{c}_{\tau_{p-1}}, \mathbf{c}_{\tau_{p-2}} \in \mathbf{R}^{p \times 1}$ , and  $\mathbf{c}_{\tau_{a-1}}, \mathbf{c}_{\tau_{a-2}} \in \mathbf{R}^{a \times 1}$  are centrifugal forces and Coriolis forces acting on the base, passive joints, and active joints. So equation (28) becomes

$$\begin{bmatrix} \mathbf{M}_b & \mathbf{M}_{bmP} & \mathbf{M}_{bmA} \\ \mathbf{M}_{mbP} & \mathbf{M}_{mPP} & \mathbf{M}_{mPA} \\ \mathbf{M}_{mbA} & \mathbf{M}_{mAP} & \mathbf{M}_{mAA} \end{bmatrix} \begin{bmatrix} \ddot{\theta}_b \\ \ddot{\theta}_P \\ \ddot{\theta}_A \end{bmatrix} + \begin{bmatrix} \mathbf{c}_b \\ \mathbf{c}_P \\ \mathbf{c}_A \end{bmatrix} \quad (29)$$

$$= \begin{bmatrix} \tau_b \\ \tau_P \\ \tau_A \end{bmatrix} = \begin{bmatrix} 0 \\ 0 \\ \tau_A \end{bmatrix},$$

where

$$\begin{bmatrix} \mathbf{c}_b \\ \mathbf{c}_p \\ \mathbf{c}_A \end{bmatrix} = \begin{bmatrix} \mathbf{c}_{\tau_{b-1}} - \mathbf{c}_{\tau_{b-2}} \\ \mathbf{c}_{\tau_{p-1}} - \mathbf{c}_{\tau_{p-2}} \\ \mathbf{c}_{\tau_{A-1}} - \mathbf{c}_{\tau_{A-2}} \end{bmatrix} \in \mathbf{R}^{(n+6) \times 1}. \quad (30)$$

Passive joints and base cannot supply torque, so  $\tau_b \equiv 0$  and  $\tau_p \equiv 0$ . If we know the motions of active joints, passive joints, and the base, the required active joint torque  $\tau_A$  can be calculated to actuate the space manipulator to arrive at the target state.

#### 4. The Analysis of Kinematic and Dynamic Coupling Relationships

Based on kinematic and dynamic models of the free-floating space manipulator with free-swinging joint failure, the kinematic and dynamic coupling relationships inside system are derived, and coupling indexes are defined to depict the coupling degree.

*4.1. Kinematic Coupling Relationships and Coupling Indexes.* For the space manipulator with free-swinging joint failure, passive joints, base, and end-effector can only be passively actuated by active joints, so we call them as “passive units” [27]. Combining them with equations (15) and (16), we have

$$\mathbf{v}_t = \begin{bmatrix} \dot{\theta}_b \\ \dot{\theta}_p \\ \mathbf{v}_e \\ \omega_e \end{bmatrix} = \begin{bmatrix} \mathbf{J}_{bA} \\ \mathbf{J}_{pA} \\ \mathbf{J}_{Pg} \end{bmatrix} \dot{\theta}_A = \mathbf{J}_t \dot{\theta}_A. \quad (31)$$

$\mathbf{v}_t \in \mathbf{R}^{(6+p+6) \times 1}$  denotes the vector consisting of all passive unit velocities, and  $\mathbf{J}_t \in \mathbf{R}^{(6+p+6) \times a}$  is the total Jacobian matrix of the system. Equation (31) reflects the kinematic coupling relationships between active joints and all passive units. For a specific task, it requires no more than a part of the passive units to move as the desired velocities in  $\mathbf{v}_t$ , so  $\mathbf{v}_t$  is the velocity of the entire task space. From equation (31), we can acquire nonhomogeneous linear equations:

$$\mathbf{J}_t \dot{\theta}_A - \mathbf{v}_t = \begin{cases} \mathbf{j}_{tr1} \dot{\theta}_A - \mathbf{v}_{t1} = 0, \\ \mathbf{j}_{tr2} \dot{\theta}_A - \mathbf{v}_{t2} = 0, \\ \vdots \\ \mathbf{j}_{tr(12+p)} \dot{\theta}_A - \mathbf{v}_{t(12+p)} = 0. \end{cases} \quad (32)$$

$\mathbf{j}_{tri}$ ,  $i = 1, 2, \dots, 12 + p$ , of  $\mathbf{J}_t$  represents the contribution of  $\dot{\theta}_A$  to  $\mathbf{v}_{ti}$ . The necessary and sufficient condition for the existence of a solution of equation (32) is  $\text{rank}(\mathbf{J}_t) = \text{rank}([\mathbf{J}_t, \mathbf{v}_t]) \leq a$ , which is equivalent to

$$\begin{cases} a \geq 12 + p, \\ \text{rank}(\mathbf{J}_t) = 12 + p. \end{cases} \quad (33)$$

It tells us that if active joints are more than passive units, and  $\mathbf{J}_t$  is full rank, we can find at least one set of solutions of  $\mathbf{J}_t \dot{\theta}_A - \mathbf{v}_t = 0$ , which means active joints can actuate all passive units at the same time. For the desired  $\mathbf{v}_t$ , we can calculate  $\dot{\theta}_A$ :

$$\dot{\theta}_A = \mathbf{J}_t^+ \mathbf{v}_t. \quad (34)$$

In particular, if  $a > 12 + p$ , the system is redundant, and equation (34) has the general solution

$$\dot{\theta}_A = \mathbf{J}_t^+ \mathbf{v}_t + (\mathbf{E}_a - \mathbf{J}_t^+ \mathbf{J}_t) \varphi, \quad (35)$$

where  $\varphi \in \mathbf{R}^{a \times 1}$  is an arbitrary vector. Equation (35) means there are infinite solutions of  $\dot{\theta}_A$  corresponding to the same  $\mathbf{v}_t$  because of the arbitrariness of  $\varphi$ . Generally speaking, redundancy empowers the space manipulator with free-swinging joint failure to perform secondary tasks, such as obstacle-avoidance, singularity-avoidance, and dexterity-optimization, as long as we find an analytical expression of  $\varphi$  according to secondary task requirements.

If conditions in equation (33) are unsatisfactory, the row vectors of  $\mathbf{J}_t$  are linearly dependent and some velocities in  $\mathbf{v}_t$  cannot be actuated by  $\dot{\theta}_A$ . In other words, the transmission efficiency from  $\dot{\theta}_A$  to  $\mathbf{v}_t$  is insufficient, corresponding to insufficiency of kinematic coupling degree. The kinematic coupling degree depends on the degree of closeness of  $\mathbf{J}_t$  to singularity, which can be represented by the minimum singular value, condition number, and manipulability. Because manipulability can reflect the general closeness to singularity, which means it can reflect the comprehensive transmission capacity from active joint motion/torque to passive units' motion. We define the kinematic coupling index based on the manipulability of  $\mathbf{J}_t$  to evaluate kinematic coupling degree.

$$w_t = \prod_{i=1}^{12+p} \sigma_i = \sqrt{\det(\mathbf{J}_t \mathbf{J}_t^T)}, \quad (36)$$

where  $\sigma_{t1} \geq \sigma_{t2} \geq \dots \geq \sigma_{t(6+p+6)} \geq 0$  are singular values of  $\mathbf{J}_t$ . When  $w_t$  is close to zeros, the transmission efficiency from  $\dot{\theta}_A$  to  $\mathbf{v}_t$  is inefficient, which means  $\mathbf{v}_t$  is kinematically uncontrollable for  $\dot{\theta}_A$ . Because  $w_t = w_t(\mathbf{q})$ , in motion planning, we should continually calculate  $w_t$  according to current state  $\mathbf{q}$ .

However, assuming at least one joint fails, so  $12 + p \geq 13$ . If we hope all passive units are controllable, the manipulator must have 14 joints at least. It is unrealistic for real space manipulators because of complicated structure and high difficulty in design. Fortunately, many space tasks only require active joints to actuate a part of passive units. We are going to discuss some typical tasks in the following.

*4.1.1. End-Effector Trajectory Tracking Task.* This task requires the end-effector to move along the predefined

trajectory to arrive at the desired position/attitude, so the task velocity vector is  $\mathbf{v}_{eA} = [\mathbf{v}_e^T, \omega_e^T]^T$ . The transmission from  $\dot{\theta}_A$  to  $\mathbf{v}_{eA}$  depends on  $\mathbf{J}_{eA}$ . When  $a \geq 6$ , the end-effector could be effectively actuated by active joints. The kinematic coupling index is defined as the manipulability of  $\mathbf{J}_{eA}$ :

$$w_{eA}(\mathbf{q}) = \prod_{i=1}^6 \sigma_{eAi} = \sqrt{\det(\mathbf{J}_{eA} \mathbf{J}_{eA}^T)}. \quad (37)$$

If  $w_{eA}(\mathbf{q})$  is close to zero,  $\mathbf{v}_{eA}$  is uncontrollable for  $\dot{\theta}_A$  and the end-effector trajectory tracking task is unrealizable. If  $w_{eA}(\mathbf{q})$  is big enough, we should interpolate  $[\mathbf{v}_e^T, \omega_e^T]^T$  to track the predefined trajectory and calculate  $\dot{\theta}_A = \mathbf{J}_{eA}^+ \mathbf{v}_{eA}$ . The manipulator can complete the task successfully with the obtained  $\dot{\theta}_A$ .

**4.1.2. Passive Joint Regulating Task.** This task requires active joints to regulate passive joints to target angles based on the first-order nonholonomic constraint between  $\dot{\theta}_A$  and  $\dot{\theta}_P$ . The task velocity vector is  $\mathbf{v}_{PA} = \dot{\theta}_P$ , and the transmission from  $\dot{\theta}_A$  to  $\dot{\theta}_P$  depends on  $\mathbf{J}_{PA}$ . When  $a \geq p$ , passive joints could be actuated by active joints. The kinematic coupling index is defined as the manipulability of  $\mathbf{J}_{PA}$ :

$$w_{PA}(\mathbf{q}) = \prod_{i=1}^p \sigma_{PAi} = \sqrt{\det(\mathbf{J}_{PA} \mathbf{J}_{PA}^T)}. \quad (38)$$

If  $w_{PA}(\mathbf{q})$  is close to zero,  $\mathbf{v}_{PA}$  is uncontrollable for  $\dot{\theta}_A$  and the passive joint regulating task is unrealizable. If  $w_{PA}(\mathbf{q})$  is big enough, we should interpolate  $\dot{\theta}_P$  according to the task requirement and calculate  $\dot{\theta}_A = \mathbf{J}_{PA}^+ \dot{\theta}_P$ .

**4.1.3. Base Position/Attitude Controlling Task.** This task requires the base to move to the desired position/attitude relying on the first-order nonholonomic constraint between  $\dot{\theta}_A$  and  $\dot{\theta}_b$ , so the task velocity vector is  $\mathbf{v}_{bA} = [\mathbf{v}_0^T, \omega_0^T]^T$ . The transmission from  $\dot{\theta}_A$  to  $\mathbf{v}_{bA}$  depends on  $\mathbf{J}_{bA}$ . When  $a \geq 6$ , the base can be actuated. The kinematic coupling index is defined as the manipulability of  $\mathbf{J}_{bA}$ :

$$w_{bA}(\mathbf{q}) = \prod_{i=1}^6 \sigma_{bAi} = \sqrt{\det(\mathbf{J}_{bA} \mathbf{J}_{bA}^T)}. \quad (39)$$

If  $w_{bA}(\mathbf{q})$  is close to zero,  $\mathbf{v}_{bA}$  is uncontrollable for  $\dot{\theta}_A$  so the task is unrealizable. If  $w_{bA}(\mathbf{q})$  is big enough, we should interpolate  $[\mathbf{v}_0^T, \omega_0^T]^T$  as the requirement and calculate  $\dot{\theta}_A = \mathbf{J}_{bA}^+ \mathbf{v}_{bA}$ .

**4.1.4. The Combination Tasks.** The space manipulator with free-swinging joint failure usually executes some combination tasks, like the task that requires active joints to actuate the end-effector to the desired position and passive joints to target angles at the same time. For this task, we select the task velocity vector as  $\mathbf{v}_{vePA} = [\mathbf{v}_e^T, \dot{\theta}_P^T]^T \in \mathbf{R}^{(3+p) \times 1}$  and the Jacobian matrix is

$$\mathbf{J}_{vePA} = \begin{bmatrix} \mathbf{J}_{eA-v} \\ \mathbf{J}_{PA} \end{bmatrix} \in \mathbf{R}^{(3+p) \times a}, \quad (40)$$

where  $\mathbf{J}_{eA-v}$  is the first three rows of  $\mathbf{J}_{eA}$ . The kinematic coupling index is the manipulability of  $\mathbf{J}_{vePA}$ . For the task to eliminate the base attitude deflection when regulating passive joints, we select the task velocity vector as  $\mathbf{v}_{wbP} = [\dot{\theta}_P^T, \omega_0^T]^T \in \mathbf{R}^{(p+3) \times 1}$  and the Jacobian matrix is

$$\mathbf{J}_{wbPA} = \begin{bmatrix} \mathbf{J}_{PA} \\ \mathbf{J}_{bA-\omega} \end{bmatrix} \in \mathbf{R}^{(p+3) \times a}, \quad (41)$$

where  $\mathbf{J}_{bA-\omega}$  is the last three row vectors of  $\mathbf{J}_{bA}$ . The kinematic coupling index is the manipulability of  $\mathbf{J}_{wbPA}$ . To eliminate base attitude disturbance, we keep  $\omega_0 \equiv 0$  [28].

For general space tasks, we should select  $\mathbf{v}_{\text{task}} = [v_{\text{task}1}, v_{\text{task}2}, \dots, v_{\text{task}f}]^T \in \mathbf{R}^{f \times 1}$  according to controlled passive units for current task requirements.  $f$  is the dimensionality of  $\mathbf{v}_{\text{task}}$ . Then, the corresponding row vectors from  $\mathbf{J}_t$  need to be taken out to construct the Jacobian matrix:

$$\mathbf{J}_{v_{\text{task}}A} = \begin{bmatrix} \mathbf{J}_{trv\_task1} \\ \mathbf{J}_{trv\_task2} \\ \vdots \\ \mathbf{J}_{trv\_taskf} \end{bmatrix} \in \mathbf{R}^{f \times a}, \quad (42)$$

and the kinematic coupling index is

$$w_{v_{\text{task}}A}(\mathbf{q}) = \prod_{i=1}^f \sigma_{v_{\text{task}}Ai} = \sqrt{\det(\mathbf{J}_{v_{\text{task}}A} \mathbf{J}_{v_{\text{task}}A}^T)}. \quad (43)$$

If  $a \geq f$  and  $w_{v_{\text{task}}A}(\mathbf{q}) > 0$ , we can interpolate  $\mathbf{v}_{\text{task}}$  as requested and calculate  $\dot{\theta}_A$  as  $\dot{\theta}_A = \mathbf{J}_{v_{\text{task}}A}^+ \mathbf{v}_{\text{task}}$ ; for  $a > f$ , the space manipulator with free-swinging joint failure is redundant for the current task, and the general solution of  $\dot{\theta}_A$  exists as

$$\dot{\theta}_A = \mathbf{J}_{v_{\text{task}}A}^+ \mathbf{v}_{\text{task}} + (\mathbf{E}_a - \mathbf{J}_{v_{\text{task}}A}^+ \mathbf{J}_{v_{\text{task}}A}) \dot{\phi}. \quad (44)$$

The analysis above depends on the conservation of system momentum. Space manipulators are usually installed on the base with large mass and inertia, such as a space station or space laboratory. The partition of Jacobian matrix is equivalent to move all passive joints to the base, so passive joints and the base make up a large combination, and all active joints make up a small combination. If system momentum is conservative, it is difficult to use a small combination to regulate a large combination. So when the base mass and inertia is large, as well as the kinematic coupling degree between active joints and passive joints, the base will be seriously inefficient. Passive joint regulation and base control tasks cannot be performed relying on motion planning.

4.2. *Dynamic Coupling Relationships and Coupling Indexes.* Expanding equation (29):

$$\mathbf{M}_b \ddot{\theta}_b + \mathbf{M}_{bmP} \ddot{\theta}_P + \mathbf{M}_{bmA} \ddot{\theta}_A + \mathbf{c}_b = 0, \quad (45)$$

$$\mathbf{M}_{mbP} \ddot{\theta}_b + \mathbf{M}_{mPP} \ddot{\theta}_P + \mathbf{M}_{mPA} \ddot{\theta}_A + \mathbf{c}_P = 0, \quad (46)$$

$$\mathbf{M}_{mbA} \ddot{\theta}_b + \mathbf{M}_{mAP} \ddot{\theta}_P + \mathbf{M}_{mAA} \ddot{\theta}_A + \mathbf{c}_A = \tau_A. \quad (47)$$

Dynamic coupling relationships inside the system can be derived from equations (45), (46), and (47).

4.2.1. *Dynamic Coupling Relationship between Active Joints and Passive Joints.* Eliminating  $\ddot{\theta}_b$  in equations (45) and (46), we have

$$\begin{aligned} -\mathbf{M}_b^{-1} \mathbf{M}_{bmP} \ddot{\theta}_P - \mathbf{M}_b^{-1} \mathbf{M}_{bmA} \ddot{\theta}_A - \mathbf{M}_b^{-1} \mathbf{c}_b \\ = -\mathbf{M}_{mbP}^+ \mathbf{M}_{mPP} \ddot{\theta}_P - \mathbf{M}_{mbP}^+ \mathbf{M}_{mPA} \ddot{\theta}_A - \mathbf{M}_{mbP}^+ \mathbf{c}_P. \end{aligned} \quad (48)$$

So

$$\ddot{\theta}_P = \mathbf{M}_{PA} \ddot{\theta}_A + \mathbf{C}_{PA}, \quad (49)$$

where  $\mathbf{M}_{PA} = (\mathbf{M}_{mbP}^+ \mathbf{M}_{mPP} - \mathbf{M}_b^{-1} \mathbf{M}_{bmP})^+ (\mathbf{M}_b^{-1} \mathbf{M}_{bmA} - \mathbf{M}_{mbP}^+ \mathbf{M}_{mPA}) \in \mathbf{R}^{p \times a}$  is the coupling inertia matrix between active joints and passive joints and  $\mathbf{C}_{PA} = (\mathbf{M}_{mbP}^+ \mathbf{M}_{mPP} - \mathbf{M}_b^{-1} \mathbf{M}_{bmP})^+ (\mathbf{M}_b^{-1} \mathbf{c}_b - \mathbf{M}_{mbP}^+ \mathbf{c}_P) \in \mathbf{R}^{p \times 1}$  is the nonlinear item. The first term in the right of equation (49) reflects the transmission from  $\ddot{\theta}_A$  to  $\ddot{\theta}_P$ , and it is the dynamic coupling relationship between active joints and passive joints. We can obtain nonhomogeneous linear equations  $\mathbf{M}_{PA} \ddot{\theta}_A + \mathbf{C}_{PA} - \ddot{\theta}_P = 0$ . If  $p \leq a$  and  $\text{rank}(\mathbf{M}_{PA}) = p$ , we have the solution of  $\ddot{\theta}_A$ . Therefore, referring to [29], the dynamic coupling index is defined as the manipulability of  $\mathbf{M}_{PA}$  to evaluate the transmission efficiency from  $\ddot{\theta}_A$  to  $\ddot{\theta}_P$ .

$$\eta_{PA}(\mathbf{q}) = \prod_{i=1}^p \varepsilon_{PAi} = \sqrt{\det(\mathbf{M}_{PA} \mathbf{M}_{PA}^T)}, \quad (50)$$

where  $\varepsilon_{PA1} \geq \varepsilon_{PA2} \geq \dots \geq \varepsilon_{PAp} \geq 0$  are singular values of  $\mathbf{M}_{PA}$ . When  $\eta_{PA}(\mathbf{q})$  is close to zero, the dynamic coupling degree between passive joints and active joints is inefficient and  $\ddot{\theta}_P$  is dynamically uncontrollable for  $\ddot{\theta}_A$ . When  $\eta_{PA}(\mathbf{q})$  is big enough, we can design the control law for  $\ddot{\theta}_P$ , and  $\ddot{\theta}_A$  which actuates the manipulator to complete the passive joint regulating task can be obtained by  $\ddot{\theta}_A = \mathbf{M}_{PA}^+ (\ddot{\theta}_P - \mathbf{C}_{PA})$ .

4.2.2. *Dynamic Coupling Relationship between Active Joints and Base.* Eliminating  $\ddot{\theta}_P$  in equations (45) and (46), we have

$$\begin{aligned} -\mathbf{M}_{bmP}^+ \mathbf{M}_b \ddot{\theta}_b - \mathbf{M}_{bmP}^+ \mathbf{M}_{bmA} \ddot{\theta}_A - \mathbf{M}_{bmP}^+ \mathbf{c}_b \\ = -\mathbf{M}_{mPP}^{-1} \mathbf{M}_{mbP} \ddot{\theta}_b - \mathbf{M}_{mPP}^{-1} \mathbf{M}_{mPA} \ddot{\theta}_A - \mathbf{M}_{mPP}^{-1} \mathbf{c}_P. \end{aligned} \quad (51)$$

So

$$\ddot{\theta}_b = \mathbf{M}_{bA} \ddot{\theta}_A + \mathbf{C}_{bA}, \quad (52)$$

where  $\mathbf{M}_{bA} = (\mathbf{M}_{mPP}^{-1} \mathbf{M}_{mbP} - \mathbf{M}_{bmP}^+ \mathbf{M}_b)^+ (\mathbf{M}_{bmP}^+ \mathbf{M}_{bmA} - \mathbf{M}_{mPP}^{-1} \mathbf{M}_{mPA}) \in \mathbf{R}^{6 \times a}$  is the coupling inertia matrix between active joints and the base.  $\mathbf{C}_{bA} = (\mathbf{M}_{mPP}^{-1} \mathbf{M}_{mbP} - \mathbf{M}_{bmP}^+ \mathbf{M}_b)^+ (\mathbf{M}_{bmP}^+ \mathbf{c}_b - \mathbf{M}_{mPP}^{-1} \mathbf{c}_P) \in \mathbf{R}^{6 \times 1}$  is the nonlinear item. The first term in the right of equation (52) is the dynamic coupling relationship between active joints and the base. The dynamic coupling index is defined as the manipulability of  $\mathbf{M}_{bA}$  to evaluate the transmission efficiency from  $\ddot{\theta}_A$  to  $\ddot{\theta}_b$ .

$$\eta_{bA}(\mathbf{q}) = \prod_{i=1}^6 \varepsilon_{bAi} = \sqrt{\det(\mathbf{M}_{bA} \mathbf{M}_{bA}^T)}. \quad (53)$$

If  $\eta_{bA}(\mathbf{q})$  is close to zero,  $\ddot{\theta}_b$  is uncontrollable for  $\ddot{\theta}_A$ . On the contrary, we can design the control law for  $\ddot{\theta}_b$  to calculate  $\ddot{\theta}_A = \mathbf{M}_{bA}^+ (\ddot{\theta}_b - \mathbf{C}_{bA})$ .

In particular, we can get transmission from  $\ddot{\theta}_A$  to  $\ddot{\theta}_b, \ddot{\theta}_P$  by combining equations (49) and (52):

$$\begin{bmatrix} \ddot{\theta}_P \\ \ddot{\theta}_b \end{bmatrix} = \begin{bmatrix} \mathbf{M}_{PA} \\ \mathbf{M}_{bA} \end{bmatrix} \ddot{\theta}_A + \begin{bmatrix} \mathbf{C}_{PA} \\ \mathbf{C}_{bA} \end{bmatrix}. \quad (54)$$

If we calculate the derivative of equation (22), we have

$$\begin{bmatrix} \dot{\ddot{\theta}}_P \\ \dot{\ddot{\theta}}_b \end{bmatrix} = \begin{bmatrix} \mathbf{J}_{PA} \\ \mathbf{J}_{bA} \end{bmatrix} \dot{\ddot{\theta}}_A + \begin{bmatrix} \dot{\mathbf{J}}_{PA} \\ \dot{\mathbf{J}}_{bA} \end{bmatrix} \ddot{\theta}_A. \quad (55)$$

Equation (55) has a similar form with equation (54), but obviously,  $\mathbf{J}_{PA} \neq \mathbf{M}_{PA}$ ,  $\mathbf{J}_{bA} \neq \mathbf{M}_{bA}$ ,  $\dot{\mathbf{J}}_{PA} \ddot{\theta}_A \neq \mathbf{C}_{PA}$ , and  $\dot{\mathbf{J}}_{bA} \ddot{\theta}_A \neq \mathbf{C}_{bA}$ , so equations (22) and (54) are different.

Equation (54) can also be derived from equations (45) and (46):

$$\begin{bmatrix} \ddot{\theta}_b \\ \ddot{\theta}_P \end{bmatrix} = - \begin{bmatrix} \mathbf{M}_b & \mathbf{M}_{bmP} \\ \mathbf{M}_{mbP} & \mathbf{M}_{mPP} \end{bmatrix}^{-1} \left( \begin{bmatrix} \mathbf{M}_{bmA} \\ \mathbf{M}_{mPA} \end{bmatrix} \ddot{\theta}_A + \begin{bmatrix} \mathbf{c}_b \\ \mathbf{c}_P \end{bmatrix} \right). \quad (56)$$

Substituting equation (56) into equation (47), we have

$$\tau_A = \mathbf{M}_{\tau A} \ddot{\theta}_A + \mathbf{C}_{\tau A}, \quad (57)$$

where

$$\begin{aligned} \mathbf{M}_{\tau A} = - \begin{bmatrix} \mathbf{M}_{mbA} & \mathbf{M}_{mAP} \end{bmatrix} \begin{bmatrix} \mathbf{M}_b & \mathbf{M}_{bmP} \\ \mathbf{M}_{mbP} & \mathbf{M}_{mPP} \end{bmatrix}^{-1} \begin{bmatrix} \mathbf{M}_{bmA} \\ \mathbf{M}_{mPA} \end{bmatrix} \\ + \mathbf{M}_{mAA} \in \mathbf{R}^{a \times a}, \end{aligned} \quad (58)$$

represents the mapping relation between  $\ddot{\theta}_A$  and  $\tau_A$  and

$$\mathbf{C}_{\tau A} = -[\mathbf{M}_{mbA} \quad \mathbf{M}_{mAP}] \begin{bmatrix} \mathbf{M}_b & \mathbf{M}_{bmP} \\ \mathbf{M}_{mbP} & \mathbf{M}_{mPP} \end{bmatrix}^{-1} \begin{bmatrix} \mathbf{c}_b \\ \mathbf{c}_P \end{bmatrix} \quad (59)$$

$$+ \mathbf{c}_A \in \mathbf{R}^{a \times 1},$$

is the nonlinear item. Equation (57) establishes the direct relation between  $\ddot{\theta}_A$  and  $\tau_A$ . After designing the control law of  $\ddot{\theta}_p$  or  $\ddot{\theta}_b$ , we can calculate  $\ddot{\theta}_A$ , and then we can obtain the torque  $\tau_A$  that actuates the manipulator. We can further find the transmission from  $\tau_A$  to  $\ddot{\theta}_p, \ddot{\theta}_b$ :

$$\begin{aligned} \ddot{\theta}_p &= \mathbf{M}_{p\tau} \tau_A + \mathbf{C}_{p\tau}, \\ \ddot{\theta}_b &= \mathbf{M}_{b\tau} \tau_A + \mathbf{C}_{b\tau}, \end{aligned} \quad (60)$$

where  $\mathbf{M}_{p\tau} = \mathbf{M}_{pA} \mathbf{M}_{\tau A}^{-1} \in \mathbf{R}^{p \times a}$ ,  $\mathbf{C}_{p\tau} = \mathbf{C}_{pA} - \mathbf{M}_{pA} \mathbf{M}_{\tau A}^{-1} \mathbf{C}_{\tau A} \in \mathbf{R}^{p \times 1}$ ,  $\mathbf{M}_{b\tau} = \mathbf{M}_{bA} \mathbf{M}_{\tau A}^{-1} \in \mathbf{R}^{6 \times a}$ , and  $\mathbf{C}_{b\tau} = \mathbf{C}_{bA} - \mathbf{M}_{bA} \mathbf{M}_{\tau A}^{-1} \mathbf{C}_{\tau A} \in \mathbf{R}^{6 \times 1}$ . So we can directly calculate  $\tau_A$  from equation (60) corresponding to the desired  $\ddot{\theta}_p$  or  $\ddot{\theta}_b$ . Dynamic coupling indexes are defined to evaluate transmission efficiency from  $\tau_A$  to  $\ddot{\theta}_p, \ddot{\theta}_b$ :

$$\begin{aligned} \eta_{p\tau}(\mathbf{q}) &= \prod_{i=1}^p \varepsilon_{p\tau i} = \sqrt{\det(\mathbf{M}_{p\tau} \mathbf{M}_{p\tau}^T)}, \\ \eta_{b\tau}(\mathbf{q}) &= \prod_{i=1}^6 \varepsilon_{b\tau i} = \sqrt{\det(\mathbf{M}_{b\tau} \mathbf{M}_{b\tau}^T)}. \end{aligned} \quad (61)$$

**4.2.3. Dynamic Coupling Relationship between Active Joints and End-Effector.** Because  $[\dot{\mathbf{v}}_e^T, \dot{\omega}_e^T]^T$  does not appear in the Lagrange equation, we cannot find a mapping relation between  $\ddot{\theta}_A$  and  $[\dot{\mathbf{v}}_e^T, \dot{\omega}_e^T]^T$  in equation (29), but we can find the dynamic coupling relationship between active joints and the end-effector from another perspective [12]. Calculating derivative of equation (16), we have

$$\begin{bmatrix} \dot{\mathbf{v}}_e \\ \dot{\omega}_e \end{bmatrix} = \mathbf{J}_{eA} \ddot{\theta}_A + \dot{\mathbf{J}}_{eA} \dot{\theta}_A. \quad (62)$$

Multiplying equation (57) by  $\mathbf{J}_{eA} \mathbf{M}_{\tau A}^{-1}$ , we have

$$\begin{aligned} \mathbf{J}_{eA} \ddot{\theta}_A + \mathbf{J}_{eA} \mathbf{M}_{\tau A}^{-1} \mathbf{C}_{\tau A} &= \mathbf{J}_{eA} \mathbf{M}_{\tau A}^{-1} \tau_A \Rightarrow \mathbf{J}_{eA} \ddot{\theta}_A + \dot{\mathbf{J}}_{eA} \dot{\theta}_A \\ &= \mathbf{J}_{eA} \mathbf{M}_{\tau A}^{-1} \tau_A + \dot{\mathbf{J}}_{eA} \dot{\theta}_A - \mathbf{J}_{eA} \mathbf{M}_{\tau A}^{-1} \mathbf{C}_{\tau A} \Rightarrow \begin{bmatrix} \dot{\mathbf{v}}_e \\ \dot{\omega}_e \end{bmatrix} \\ &= \mathbf{M}_{e\tau} \tau_A + \mathbf{C}_{e\tau}, \end{aligned} \quad (63)$$

where  $\mathbf{M}_{e\tau} = \mathbf{J}_{eA} \mathbf{M}_{\tau A}^{-1} \in \mathbf{R}^{6 \times a}$  is the coupling inertia matrix representing the transmission from  $\tau_A$  to  $[\dot{\mathbf{v}}_e^T, \dot{\omega}_e^T]^T$  and  $\mathbf{C}_{e\tau} = \dot{\mathbf{J}}_{eA} \dot{\theta}_A - \mathbf{J}_{eA} \mathbf{M}_{\tau A}^{-1} \mathbf{C}_{\tau A} \in \mathbf{R}^{6 \times 1}$  is the nonlinear item. Equation (63) is the dynamic coupling relationship between active joints and the end-effector. The dynamic coupling index between active joints and the end-effector is the manipulability of  $\mathbf{M}_{e\tau}$ :

$$\eta_{e\tau}(\mathbf{q}) = \prod_{i=1}^6 \varepsilon_{e\tau i} = \sqrt{\det(\mathbf{M}_{e\tau} \mathbf{M}_{e\tau}^T)}. \quad (64)$$

If  $\eta_{e\tau}(\mathbf{q})$  is close to zero,  $[\dot{\mathbf{v}}_e^T, \dot{\omega}_e^T]^T$  is uncontrollable for  $\tau_A$ . On the contrary, we can design the control law for  $[\dot{\mathbf{v}}_e^T, \dot{\omega}_e^T]^T$  to calculate

$$\tau_A = \mathbf{M}_{e\tau}^+ \left( \begin{bmatrix} \dot{\mathbf{v}}_e \\ \dot{\omega}_e \end{bmatrix} - \mathbf{C}_{e\tau} \right). \quad (65)$$

Equations (60) and (63) can be reduced to the following constraints:

$$\begin{aligned} \mathbf{g}_1(\ddot{\theta}_b, \ddot{\theta}_A \text{ or } \tau_A, t) &= 0, \\ \mathbf{g}_2(\ddot{\theta}_b, \ddot{\theta}_A \text{ or } \tau_A, t) &= 0, \\ \mathbf{g}_3(\dot{\mathbf{v}}_e, \dot{\omega}_e, \tau_A, t) &= 0. \end{aligned} \quad (66)$$

**Theorem.** The constraints in equation (70) are also nonholonomic.

*Proof.* Taking equation (49) as an example, we have

$$\mathbf{M}_{pA} \ddot{\theta}_A - \ddot{\theta}_p + \mathbf{C}_{pA} = 0 \Rightarrow [0_{p \times 6} \quad -\mathbf{E}_{p \times p} \quad \mathbf{M}_{pA}] \ddot{\mathbf{q}} + \mathbf{C}_{pA} = 0, \quad (67)$$

making  $\mathbf{M}_{sPA} = [0_{p \times 6} \quad -\mathbf{E}_{p \times p} \quad \mathbf{M}_{pA}] \in \mathbf{R}^{p \times (6+n)}$ . Assuming there exists the first-order constraint  $\mathbf{p}(\mathbf{q}, \dot{\mathbf{q}}) = 0$  whose derivative with respect to time is

$$\frac{d\mathbf{p}}{dt} = \frac{\partial \mathbf{p}}{\partial \mathbf{q}} \dot{\mathbf{q}} + \frac{\partial \mathbf{p}}{\partial \dot{\mathbf{q}}} \ddot{\mathbf{q}}. \quad (68)$$

Assuming constraint in equation (66) is holonomic, we have

$$\begin{cases} \frac{\partial \mathbf{p}}{\partial \dot{\mathbf{q}}} \dot{\mathbf{q}} = \mathbf{C}_{pA}, \\ \frac{\partial \mathbf{p}}{\partial \mathbf{q}} = \mathbf{M}_{sPA}. \end{cases} \quad (69)$$

Considering  $\dot{\mathbf{q}} = 0$ , we can obtain the general solution of  $\mathbf{p}(\mathbf{q}, \dot{\mathbf{q}})$ :

$$\mathbf{p}(\mathbf{q}, \dot{\mathbf{q}}) = \mathbf{M}_{sPA} \dot{\mathbf{q}} + \mathbf{s}(\mathbf{q}) + \mathbf{C} = 0. \quad (70)$$

$\mathbf{s}(\mathbf{q})$  is relative to the state variable  $\mathbf{q}$ .  $\mathbf{C}$  is a constant vector. The derivative of equation (70) is

$$\frac{d\mathbf{p}}{dt} = \mathbf{M}_{sPA} \ddot{\mathbf{q}} + \dot{\mathbf{M}}_{sPA} \dot{\mathbf{q}} + \frac{d\mathbf{s}}{d\mathbf{q}} \dot{\mathbf{q}} = 0. \quad (71)$$

Substituting  $\mathbf{c}_b$  and  $\mathbf{c}_p$  into equation (71), and comparing it with equation (67), we obtain

$$\begin{cases} \frac{d\mathbf{s}}{d\mathbf{q}} = \mathbf{M}_1 [\dot{\mathbf{M}}_b & \dot{\mathbf{M}}_{bmP} & \dot{\mathbf{M}}_{bmA}] - \mathbf{M}_2 [\dot{\mathbf{M}}_{mbP} & \dot{\mathbf{M}}_{mPP} & \dot{\mathbf{M}}_{mPA}] - \dot{\mathbf{M}}_{sPA}, \\ \frac{\partial \mathbf{M}}{\partial \mathbf{q}_P} = \frac{\partial \mathbf{M}}{\partial \mathbf{q}_b}. \end{cases} \quad (73)$$

$\mathbf{s}(\mathbf{q})$  is only relative to  $\mathbf{q}$  instead of  $\dot{\mathbf{q}}$ , so the first equality is not satisfied. The second equality is also not satisfied because  $\theta_p$  and  $\theta_b$  are not cyclic coordinates in  $\mathbf{M}$ . Therefore,  $\mathbf{p}(\mathbf{q}, \dot{\mathbf{q}}) = 0$  does not exist and the constraints in equation (66) are nonholonomic. Because equation (66) is the constraints among the second-order derivatives of  $\theta_b, \theta_A, \theta_p, \mathbf{p}_e, \Psi_e$ , they are called as the second-order nonholonomic constraint.

The free-floating space manipulator with free-swinging joint failure simultaneously contains the first-order nonholonomic constraint and the second-order nonholonomic constraint, and they are independent with each other. From a mathematical viewpoint, equations (17) and (66) belong to differential equations, and they have the same solution. In fact, because null space exists in equation (14), we can find the same solution to these two differential equations. Therefore, motions of the free-floating space manipulator with free-swinging joint failure simultaneously satisfy the first-order and second-order nonholonomic constraints.

The analysis above is not based on conservation of system momentum, so even if base mass and inertia are very large, the degree of dynamic coupling may be large enough to enable active joints to actuate passive units through the control method.

In summary, dynamic coupling relationship between active joints and all passive units is

$$\begin{aligned} \mathbf{a}_{bP} &= \begin{bmatrix} \ddot{\theta}_b \\ \ddot{\theta}_p \end{bmatrix} = \mathbf{M}_{bP} \ddot{\theta}_A + \mathbf{C}_{bP}, \\ \text{or } \mathbf{a}_t &= \begin{bmatrix} \ddot{\theta}_b \\ \ddot{\theta}_p \\ \dot{\mathbf{v}}_e \\ \dot{\omega}_e \end{bmatrix} = \mathbf{M}_{t\tau} \tau_A + \mathbf{C}_{t\tau}. \end{aligned} \quad (74)$$

$$\begin{aligned} &\left\{ \mathbf{M}_1 [\dot{\mathbf{M}}_b \quad \dot{\mathbf{M}}_{bmP} \quad \dot{\mathbf{M}}_{bmA}] - \mathbf{M}_2 [\dot{\mathbf{M}}_{mbP} \quad \dot{\mathbf{M}}_{mPP} \quad \dot{\mathbf{M}}_{mPA}] \right. \\ &\quad \left. - \dot{\mathbf{M}}_{sPA} - \frac{d\mathbf{s}}{d\mathbf{q}} \right\} \dot{\mathbf{q}} + \frac{1}{2} \dot{\mathbf{q}}^T \left( \frac{\partial \mathbf{M}}{\partial \mathbf{q}_P} - \frac{\partial \mathbf{M}}{\partial \mathbf{q}_b} \right) \dot{\mathbf{q}} = 0. \end{aligned} \quad (72)$$

where  $\mathbf{M}_1 = (\mathbf{M}_{mbP}^+ \mathbf{M}_{mPP} - \mathbf{M}_b^{-1} \mathbf{M}_{bmP})^+ \mathbf{M}_b^{-1}$  and  $\mathbf{M}_2 = (\mathbf{M}_{mbP}^+ \mathbf{M}_{mPP} - \mathbf{M}_b^{-1} \mathbf{M}_{bmP})^+ \mathbf{M}_{mbP}^+$ . To satisfy the above equality, we have

$\mathbf{a}_t \in \mathbf{R}^{(p+12) \times 1}$  is the acceleration of the entire task space.

$$\mathbf{M}_{bP} = \begin{bmatrix} \mathbf{M}_{bA} \\ \mathbf{M}_{PA} \end{bmatrix} \in \mathbf{R}^{(p+6) \times a}, \quad (75)$$

is the coupling inertia matrix representing the transmission from  $\ddot{\theta}_A$  to  $[\ddot{\theta}_b^T, \ddot{\theta}_p^T]^T$ , and

$$\mathbf{M}_{t\tau} = \begin{bmatrix} \mathbf{M}_{b\tau} \\ \mathbf{M}_{P\tau} \\ \mathbf{M}_{e\tau} \end{bmatrix} \in \mathbf{R}^{(p+12) \times a}, \quad (76)$$

is the coupling inertia matrix representing the transmission from  $\tau_A$  to  $\mathbf{a}_t$ .

$$\begin{aligned} \mathbf{C}_{bP} &= \begin{bmatrix} \mathbf{C}_{bA} \\ \mathbf{C}_{PA} \end{bmatrix} \in \mathbf{R}^{(p+6) \times 1}, \\ \mathbf{C}_{t\tau} &= \begin{bmatrix} \mathbf{C}_{b\tau} \\ \mathbf{C}_{P\tau} \\ \mathbf{C}_{e\tau} \end{bmatrix} \in \mathbf{R}^{(p+12) \times 1}, \end{aligned} \quad (77)$$

are nonlinear items. Based on dynamic coupling relationships, active joints can actuate the manipulator to execute tasks as the same as motion planning. For general tasks, we should select the task acceleration vector  $\mathbf{a}_{\text{task}} \in \mathbf{R}^{f \times 1}$  according to task requirements and construct  $\mathbf{M}_{a_{\text{task}}A} \in \mathbf{R}^{f \times a}$  and  $\mathbf{C}_{a_{\text{task}}A} \in \mathbf{R}^{f \times 1}$ . Then, we design the control law for  $\mathbf{a}_{\text{task}}$

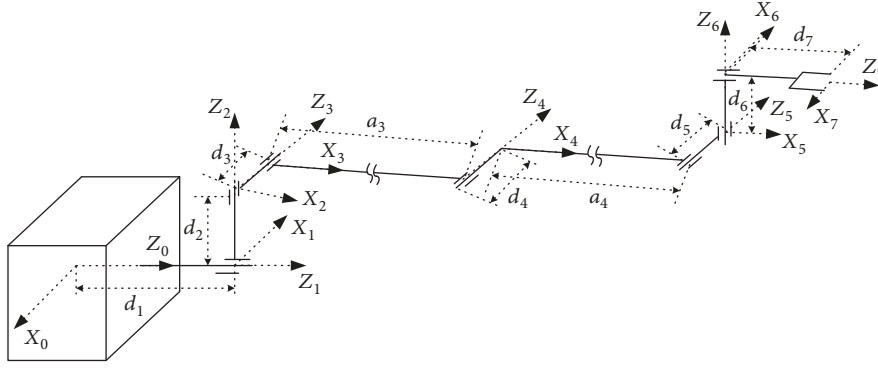


FIGURE 2: SSRMS-type 7 DOF space manipulator.

to guarantee that the selected passive units will converge to the equilibrium point, and  $\tau_A$  is obtained. If  $a > f$ , the space manipulator is redundant and the solutions of  $\ddot{\theta}_A$  and  $\tau_A$  are

$$\begin{aligned} \ddot{\theta}_A &= \mathbf{M}_{a_{\text{task}}A}^+ (\mathbf{a}_{\text{task}} - \mathbf{C}_{a_{\text{task}}A}) + (\mathbf{I} - \mathbf{M}_{a_{\text{task}}A}^+ \mathbf{M}_{a_{\text{task}}A}) \zeta, \\ \text{or } \tau_A &= \mathbf{M}_{a_{\text{task}}A}^+ (\mathbf{a}_{\text{task}} - \mathbf{C}_{a_{\text{task}}A}) + (\mathbf{I} - \mathbf{M}_{a_{\text{task}}A}^+ \mathbf{M}_{a_{\text{task}}A}) \zeta. \end{aligned} \quad (78)$$

$\zeta \in \mathbf{R}^{a \times 1}$  is an arbitrary vector. Appropriately designing  $\zeta$ , the manipulator can perform primary and secondary tasks at the same time.

**4.3. Global Kinematic and Dynamic Coupling Indexes.** The kinematic and dynamic coupling indexes defined above are with respect to system state variables  $\mathbf{q}$ . If their values are large, it only indicates that motion transmission efficiency from active joints to passive units is high only at the current  $\mathbf{q}$ , so the indexes above are called as local indexes for kinematic and dynamic coupling in state space. However, before structure design, motion planning, and controller design, the system state is unknown, so the local coupling indexes are not appropriate at this moment. We care more about the global coupling degree in the entire state space, and global kinematic and dynamic coupling indexes are defined as

$$\begin{aligned} w_*^g &= \frac{\int_{\mathbf{q}} w_*^g(\mathbf{q}) d\mathbf{q}}{\int_{\mathbf{q}} d\mathbf{q}}, \\ \eta_*^g &= \frac{\int_{\mathbf{q}} \eta_*^g(\mathbf{q}) d\mathbf{q}}{\int_{\mathbf{q}} d\mathbf{q}}. \end{aligned} \quad (79)$$

$w_*$  and  $w_*^g$  correspond to local and global manipulability of a Jacobian matrix  $\mathbf{J}_*$ , respectively.  $\eta_*$  and  $\eta_*^g$  correspond to local and global manipulability of an inertia matrix  $\mathbf{M}_*$ , respectively. If kinematic and dynamic parameters are determined, global indexes can be calculated. The higher the values of global indexes, the higher the motion transmission efficiency from active joints to passive units whatever state the manipulator is in. If selecting different healthy joints as active joints, different values of global indexes will be obtained. There exists the case that values of global indexes

TABLE 1: Kinematic parameters of SSRMS-type 7 DOF space manipulator.

Joint no.	Torsion angle $\alpha_{i-1}$ (°)	Link length $a_{i-1}$ (m)	Joint angle $\theta_i$ (°)	Link offset $d_i$ (m)
1	0	0	180	1.1
2	-90	0	-90	0.5
3	-90	0	0	0.5
4	0	5	0	0.5
5	0	5	0	0.5
6	90	0	90	0.5
7	90	0	180	1.1

TABLE 2: Dynamic parameters of SSRMS-type 7 DOF space manipulator.

Joint no.	Link mass $m_i$ (kg)	Link inertia $m$ diag $[I_{xxi}, I_{yyi}, I_{zzi}]$ (kg·m <sup>2</sup> )	Link centroid position $P_{cii}$ (m)
0	$10^6$	Diag $[10^6, 10^6, 10^6]$	$[0, 0, 0]^T$
1	42.5	Diag $[0.8854, 0.0531, 0.8854]$	$[0, 0.25, 0]^T$
2	42.5	Diag $[0.8854, 0.0531, 0.8854]$	$[0, 0.25, 0]^T$
3	70	Diag $[0.0875, 145.8333, 145.8333]$	$[2.5, 0, 0]^T$
4	70	Diag $[0.0875, 145.8333, 145.8333]$	$[2.5, 0, 0]^T$
5	42.5	Diag $[0.8854, 0.8854, 0.0531]$	$[0, 0, 0.25]^T$
6	42.5	Diag $[0.8854, 0.8854, 0.0531]$	$[0, 0, 0.25]^T$
7	42.5	Diag $[1.2750, 1.2750, 0.0531]$	$[0, 0, 0.55]^T$

are close whether we select some healthy joints. It indicates that these joints are incapable to actuate passive units, so we should not select them as active joints.

## 5. Simulation Experiments

In simulation, we plan motions for the space manipulator with free-swing joint failure to perform some tasks to verify the existence and correctness of the first-order nonholonomic constraint. Then, we give a study case for calculating kinematic and dynamic indexes and discuss the variation of  $w_{PA}^g$  and  $\eta_{PA}^g$  with the increasing base mass and inertia. In

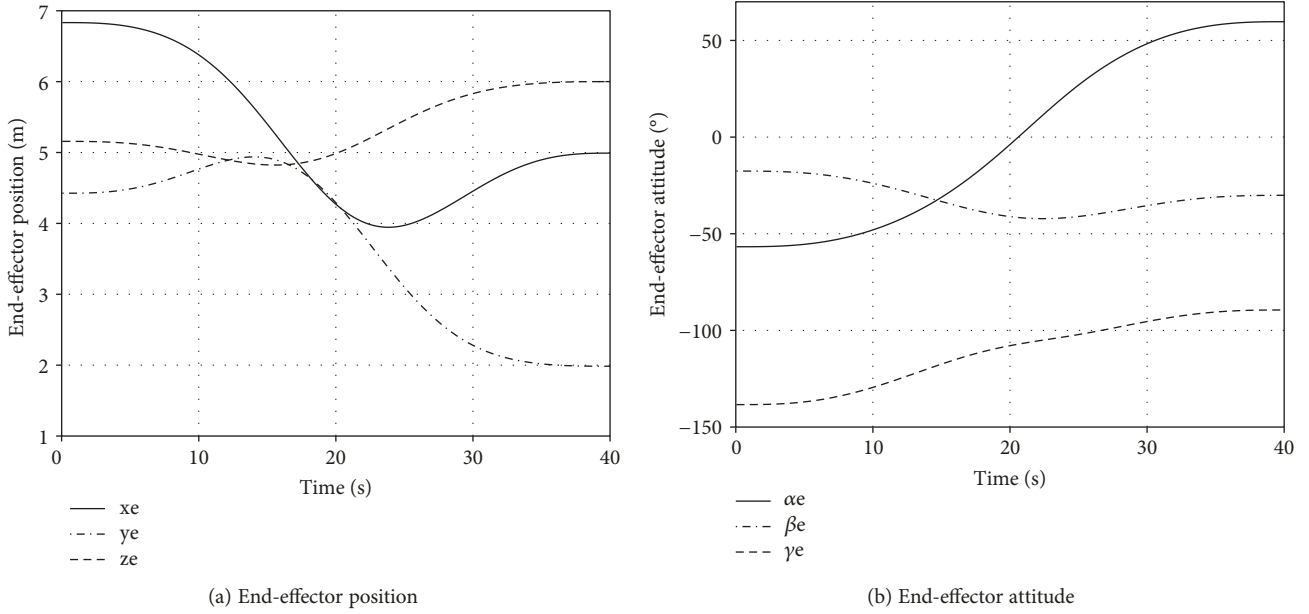


FIGURE 3: The variation of  $[\mathbf{x}_e^T, \Psi_e^T]^T$  with execution of the trajectory tracking task.

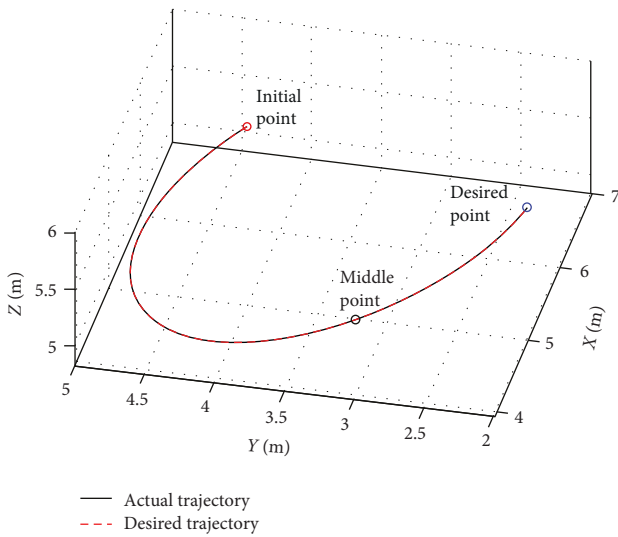


FIGURE 4: Comparison between the actual and desired end-effector trajectory.

particular, aiming at the case where a passive regulating task cannot be completed through motion planning with large base mass and inertia, we design the control law based on PD controller for  $\ddot{\theta}_p$ , and the task is completed based on the second-order nonholonomic constraint. The practicability of the coupling index and correctness of the second-order nonholonomic constraint are verified.

Simulation experiments are carried out surrounding SSRMS-type 7 DOF space manipulator in Figure 2. Its kinematic and dynamic parameters are in Tables 1 and 2.

**5.1. Motion Planning for the Space Manipulator with Free-Swinging Joint Failure.** Aiming at the end-effector trajectory tracking and passive joint regulating tasks and the combination tasks that track end-effector trajectory and limit base

attitude deflection when regulating passive joints, we plan motions for the space manipulator based on the first-order nonholonomic constraint. The existence of the first-order nonholonomic constraint is verified, and the motion planning based on kinematic coupling relationships is applied.

**5.1.1. End-Effector Trajectory Tracking Task.** For the SSRMS-type space manipulator with the single joint failure, it has 6 healthy joints. Selecting all healthy joints as active joints, the end-effector trajectory tracking task can be performed. Assuming the first joint fails, the setting initial manipulator configuration is  $\theta_{ini} = [-50^\circ, -170^\circ, 150^\circ, -60^\circ, 130^\circ, 170^\circ, 0^\circ]^T$  and the initial base position/attitude is  $\theta_{b\_ini} = [0, 0, 0, 0, 0, 0]^T$ . The task requires the end-effector to move along an arc trajectory to position/attitude  $[\mathbf{x}_{e\_des}^T, \Psi_{e\_des}^T]^T = [5\text{ m}, 2\text{ m}, 6\text{ m}, 60^\circ, -30^\circ, -90^\circ]^T$  and pass the middle point  $\mathbf{x}_{e\_mid} = [4\text{ m}, 3\text{ m}, 5.5\text{ m}]^T$ . Task execution time is 40 s. We interpolate the velocity of the end-effector with the quartic polynomial

$$v(t) = 1.0734e^{-6}t^4 - 8.5874e^{-5}t^3 + 1.7175e^{-3}t^2. \quad (80)$$

The variation of  $[\mathbf{x}_e^T, \Psi_e^T]^T = [x_e, y_e, z_e, \alpha_e, \beta_e, \gamma_e]^T$  is in Figure 3, and the comparison between the actual and the desired end-effector trajectory is in Figure 4.

The joint motion is shown in Figure 5.

As can be seen from Figures 3–5, end-effector moves along the desired trajectory to arrive at the desired position/attitude, and the joint motion is smooth, so the end-effector trajectory tracking task is accomplished based on motion planning. Velocity of the passive first joint is calculated from equation (15), and its angle is obtained by integral.

**5.1.2. Passive Joint Regulating Task.** If the number of passive joints is less than or equal to 3, there will be at least 4 healthy

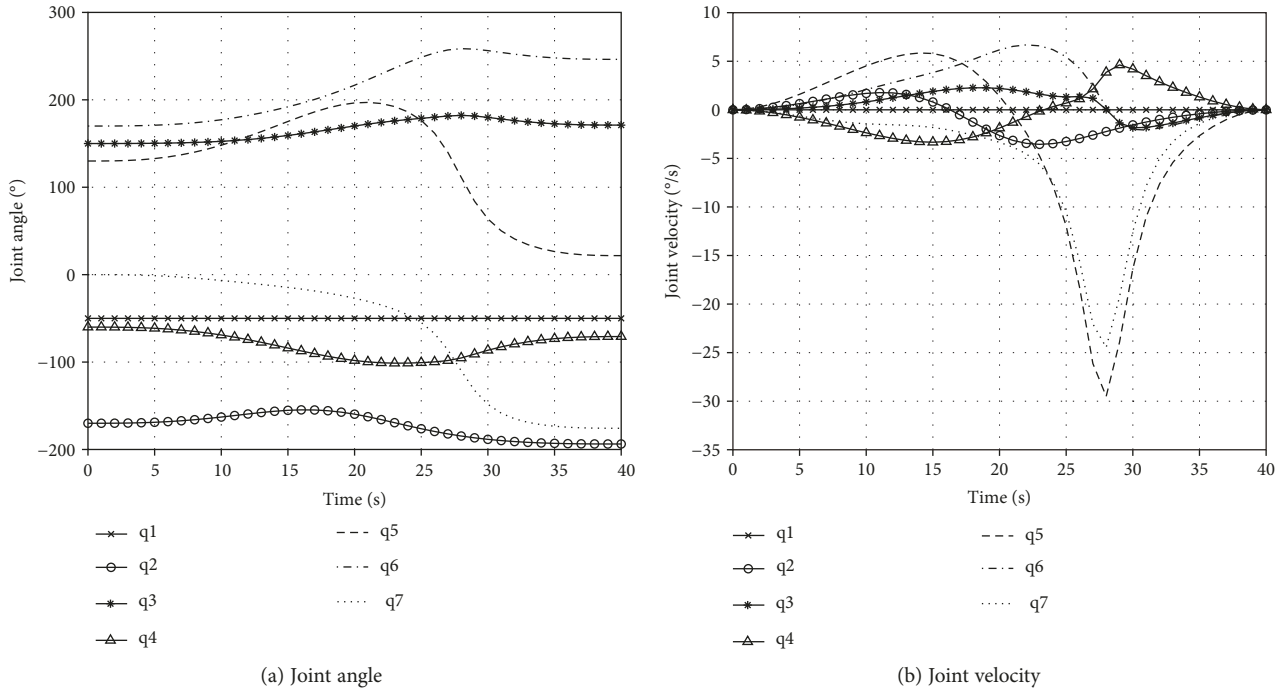


FIGURE 5: The variations of joint angle and velocity with execution of the trajectory tracking task.

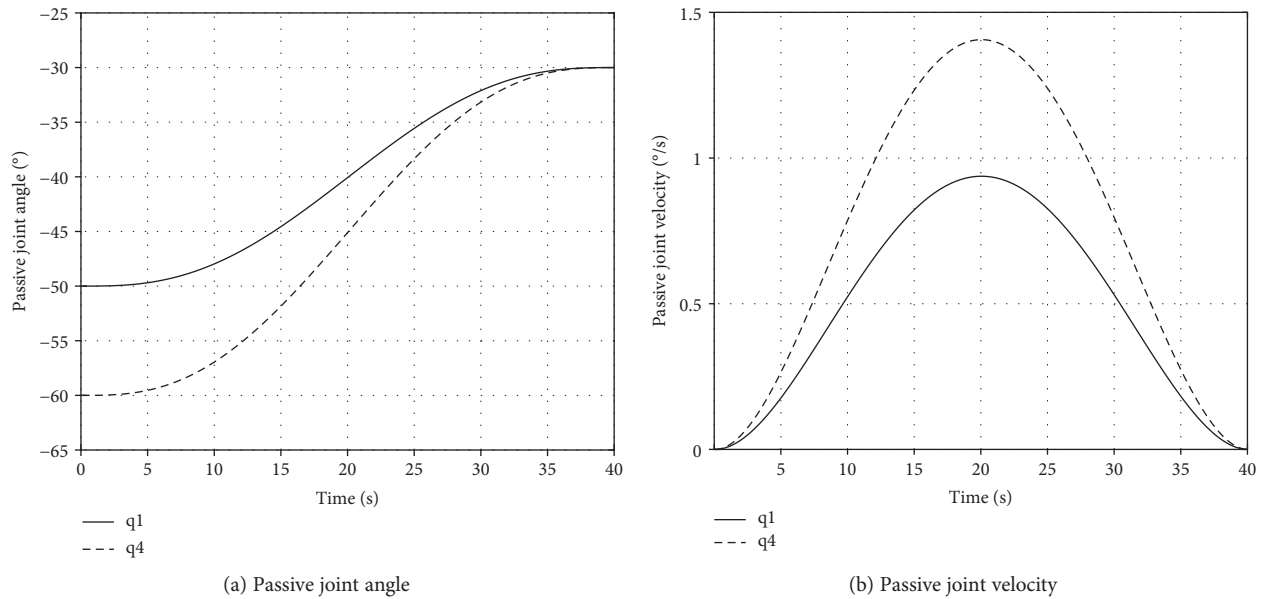


FIGURE 6: The variations of passive joint angle and velocity with execution of the passive joint regulating task.

joints and the manipulator can perform passive joint regulating task. Assuming the first and fourth joints fail, the initial configuration is  $\theta_{ini} = [-50^\circ, -170^\circ, 150^\circ, -60^\circ, 130^\circ, 170^\circ, 0^\circ]^T$  and the initial base position/attitude is  $\theta_{b\_ini} = [0, 0, 0, 0, 0, 0]^T$ . The task requires all passive joints to be regulated to  $\theta_{P\_des} = [-30^\circ, -30^\circ]^T$  in 40 s. However, for the base mass and inertia in Table 2, active joints cannot regulate passive joints because the kinematic coupling degree is seriously insufficient. Therefore, we reset the base mass as  $m_0 = 100 \text{ kg}$  and inertia as  $I_0 = \text{diag} [100 \text{ kg} \cdot \text{m}^2, 100 \text{ kg} \cdot \text{m}^2,$

$100 \text{ kg} \cdot \text{m}^2]$ . Interpolating  $\dot{\theta}_p$  with the quartic polynomial, variations of  $\theta_p$  and  $\dot{\theta}_p$  are shown in Figure 6.

Variations of  $\theta_A$  and  $\dot{\theta}_A$  are shown in Figure 7.

It can be seen that two passive joints are regulated to  $-30^\circ$  in 40 s and the motion of active joints is smooth, so the passive joint regulating task is accomplished.

5.1.3. *Tracking End-Effector Trajectory When Regulating Passive Joints.* If the number of passive joints is less than or equal to 2, there will be at least 5 healthy joints, and active

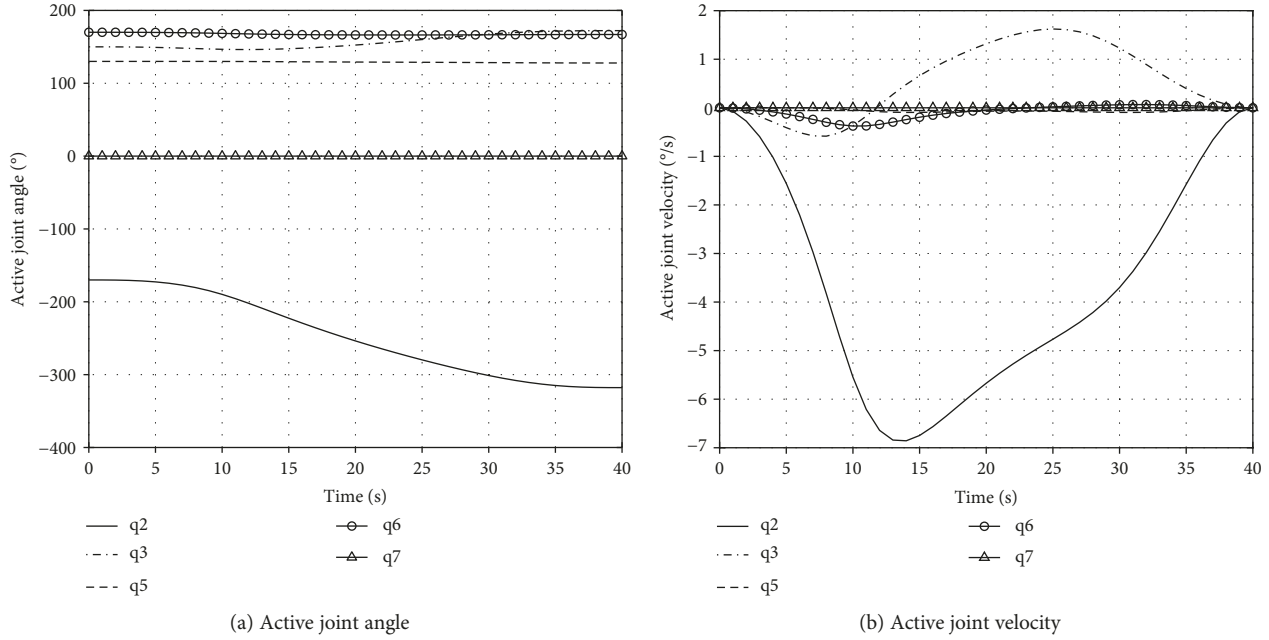


FIGURE 7: The variations of active joint angle and velocity with execution of the passive joint regulating task.

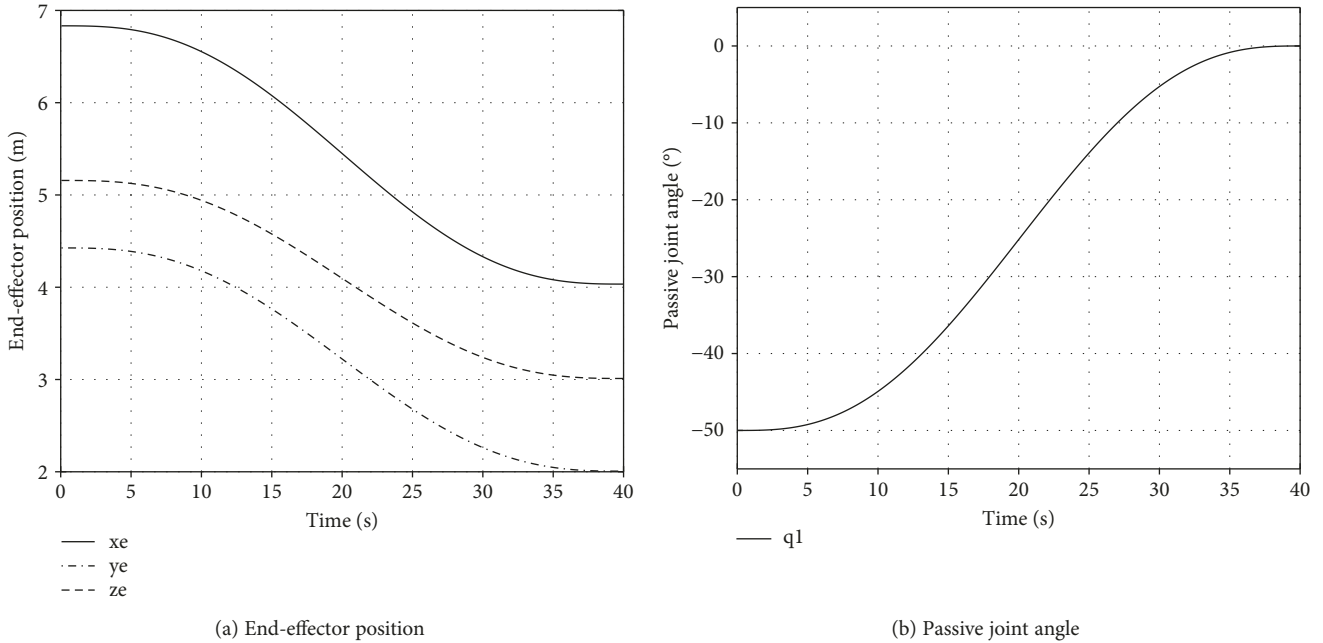


FIGURE 8: The variations of the end-effector position and passive joint angle with execution of the combination task.

joints can actuate the end-effector to the desired position and regulate passive joints to target angles simultaneously. Assuming the first joint fails, the initial configuration is  $\theta_{ini} = [-50^\circ, -170^\circ, 150^\circ, -60^\circ, 130^\circ, 170^\circ, 0^\circ]^T$  and initial base position/attitude is  $\theta_{b\_ini} = [0, 0, 0, 0, 0, 0]^T$ . The task requires the end-effector to track a straight trajectory to the desired position  $\mathbf{x}_{e\_des} = [4\text{ m}, 2\text{ m}, 3\text{ m}]^T$  and the passive joints to be regulated to  $\theta_{p\_des} = 0^\circ$  in 40 s. Base mass and inertia are the same with the passive regulating task. Variations of  $\mathbf{x}_e$  and  $\theta_p$  are in Figure 8. The comparison between the actual and the desired trajectory is in Figure 9.

The end-effector arrives at the desired position, and the passive joint is regulated to the target angle in 40 s, so the combination task is accomplished.

**5.1.4. Limiting Base Attitude Deflection When Regulating Passive Joints.** If the number of passive joints is less than or equal to 2, active joints can eliminate base attitude deflection when regulating passive joints. Assuming the first joint fails, the initial configuration is  $\theta_{ini} = [-50^\circ, -170^\circ, 150^\circ, -60^\circ, 130^\circ, 170^\circ, 0^\circ]^T$  and the initial base position/attitude is  $\theta_{b\_ini} = [0, 0, 0, 0, 0, 0]^T$ . The task requires the passive joint

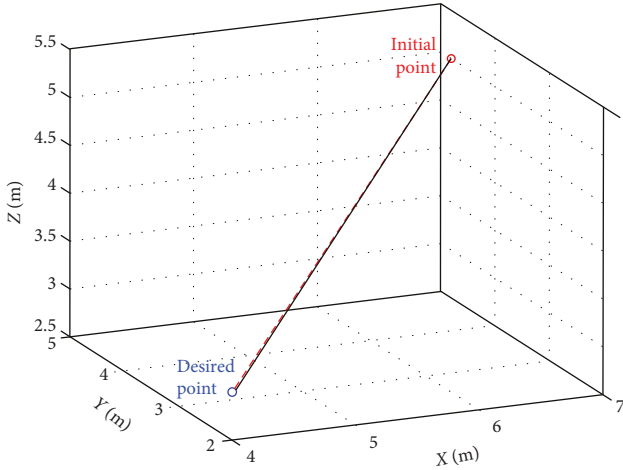


FIGURE 9: Comparison between the actual and the desired end-effector trajectory for the combination task.

to be regulated to  $\theta_{p\_des} = 0^\circ$ , and base attitude is not disturbed. Base mass and inertia are also the same with the passive regulating task. Variations of  $\theta_p$  and  $\theta_b$  are in Figure 10.

Figure 10 shows that the passive joint converges to  $0^\circ$  in 40 s and the order of magnitudes of base attitude deflection is only  $10^{-11}$ , so the combination task is accomplished.

During task execution, the values of kinematic coupling indexes are large enough, or else the tasks cannot be accomplished. The simulation results above tell us the space manipulator can execute many typical tasks based on motion planning, which verifies the existence and correctness of the first-order nonholonomic constraint inside the system.

**5.2. Calculation and Application Example for Kinematic and Dynamic Coupling Indexes.** Aiming at the space manipulator in Figure 2 with free-swinging first joint failure, we give an example for calculating local and global kinematic and dynamic coupling indexes and discuss the differences of values of coupling indexes when selecting different healthy joints as active joints. Then, we analyze the variations of  $w_{PA}^g$  and  $\eta_{PA}^g$  with the increasing base mass and inertia in particular and point out that when the base mass and inertia are large, passive joint regulation and base deflection limitation cannot be realized through motion planning. In particular, aiming at the passive joint regulating task, we design the control law for  $\dot{\theta}_p$  based on PD controller and calculate  $\tau_A$  to actuate the manipulator to complete the task.

**5.2.1. Calculation of Coupling Indexes.** Setting the configuration as  $\theta = [-50^\circ, -170^\circ, 150^\circ, -60^\circ, 130^\circ, 170^\circ, 0^\circ]^T$ , the base position/attitude is  $\theta_b = [0, 0, 0, 0, 0, 0]^T$ , the base mass is  $m_0 = 100$  kg, and the base inertia is  $I_0 = \text{diag} [100 \text{ kg} \cdot \text{m}^2, 100 \text{ kg} \cdot \text{m}^2, 100 \text{ kg} \cdot \text{m}^2]$ . Assuming that the rotation range of every joint is  $[\theta_{i\_min}, \theta_{i\_max}] = [-180^\circ, 180^\circ]$ ,  $i = 1, 2, \dots, 7$ , the base position deflection limitation is  $[x_{0j\_min}, x_{0j\_max}] = [-1 \text{ m}, 1 \text{ m}]$ ,  $j = 1, 2, 3$  and the attitude deflection limitation is  $[\Psi_{0k\_min}, \Psi_{0k\_max}] = [-20^\circ, 20^\circ]$ ,  $k = 1, 2, 3$ . For the space manipulator with free-swinging first joint failure in Figure 2, selecting all healthy joints as active joints,

we calculate the kinematic and dynamic coupling indexes in Table 3.

In Table 3, we make the value which is less than  $10^{-40}$  equal to zero. Thus, the dynamic coupling degree between active joints and the base is insufficient. In particular, if we lock the fourth and seventh joints, and select other healthy joints as active joints, kinematic and dynamic coupling indexes turn into what is found in Table 4.

As can be seen from Table 4, active joints without the fourth and seventh joints are incapable of actuating the end-effector or controlling the base because the number of active joints is less than the DOF of the end-effector and base. However, values of  $w_{PA}$ ,  $\eta_{PA}$ , and  $\eta_{P\tau}$  in Tables 3 and 4 are similar, especially for global indexes, so active joints without the fourth and seventh joints can still regulate passive joints.

The global indexes can not only depict the motion transmission efficiency from active joints to passive units but also serve as the reference to reducing the number of active joints. Users can select the fewest active joints with enough coupling degree to actuate the manipulator.

**5.2.2. Effect of Base Mass and Inertia on  $w_{PA}^g$  and  $\eta_{PA}^g$ .** Making base mass and inertia are

$$m_0 = m_c, \quad I_0 = \begin{bmatrix} m_c & 0 & 0 \\ 0 & m_c & 0 \\ 0 & 0 & m_c \end{bmatrix}. \quad (81)$$

$m_c$  is the equivalent mass of the base [30]. We set the values of  $m_c$  as  $m_c \in \{10^1, 10^2, 10^3, 10^4, 10^5, 10^6, 10^7\}$  kg. Assuming the first joint fails and selecting all healthy joints as active joints and taking  $\lg m_c$  as the  $x$ -axis, we draw the figures to exhibit the variation of  $w_{PA}^g$  and  $\eta_{PA}^g$  with  $m_c$  in Figure 11.

With increase of the base mass and inertia,  $w_{PA}^g$  and  $\eta_{PA}^g$  decrease continually. When  $m_c > 10^6$ , the value of  $w_{PA}^g$  reduces to  $10^{-8}$  and the magnitudes of change in  $w_{PA}^g$  reach up to  $10^7$ . But value of  $\eta_{PA}^g$  stabilizes around 1.4, and the magnitudes of change in  $\eta_{PA}^g$  are only  $10^1$ . Thus, active joints cannot effectively regulate passive joints based on motion planning, but can regulate passive joints based on the control method at this moment.

We design the control method to regulate passive joints based on the second-order nonholonomic constraint. We make  $\theta_{p\_des} = -30^\circ$ ,  $\dot{\theta}_{p\_des} = 0^\circ/\text{s}$ , and  $\ddot{\theta}_{p\_des} = 0^\circ/\text{s}^2$  as the desired states of passive joints and design the PD controller for  $\dot{\theta}_p$ :

$$\ddot{\theta}_p = \ddot{\theta}_{p\_des} + K_D(\dot{\theta}_{p\_des} - \dot{\theta}_p) + K_P(\theta_{p\_des} - \theta_p). \quad (82)$$

Making  $\mathbf{e} = \theta_{p\_des} - \theta_p$ , we have  $\ddot{\mathbf{e}} + K_D\dot{\mathbf{e}} + K_P\mathbf{e} = 0$ . According to the characteristic of the second-order homogeneous differential equation,  $\mathbf{e}$  exponentially converges to

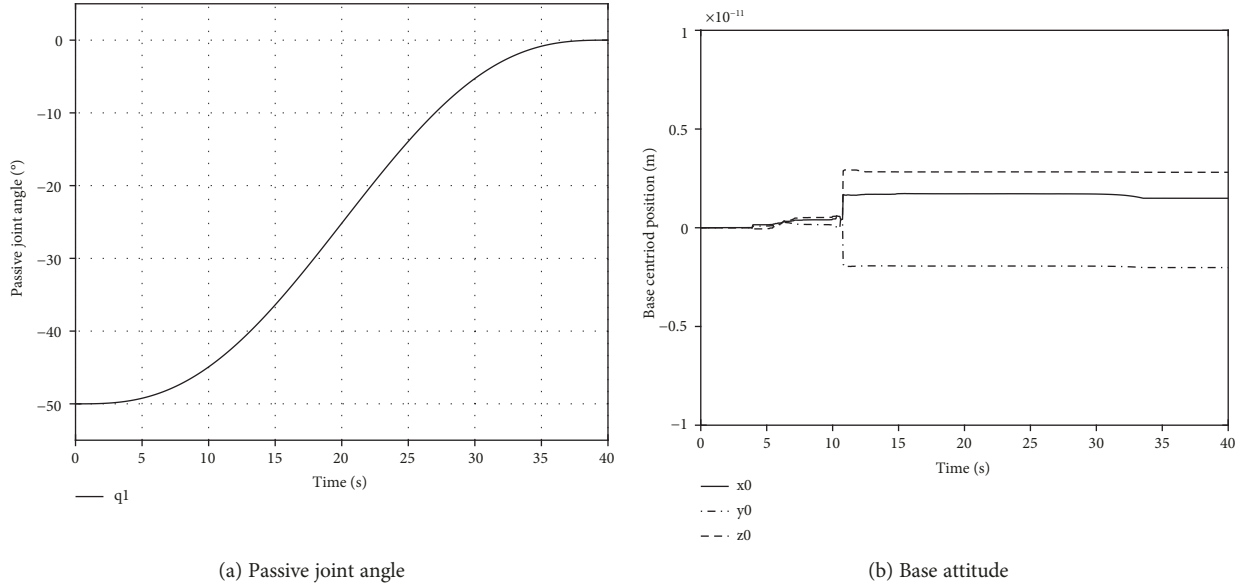


FIGURE 10: The variations of passive joint angle and base attitude with execution of the combination task.

TABLE 3: Kinematic and dynamic coupling indexes.

	Single	Local value Maximum	Minimum	Global value
$w_{eA}$	0.0016	1.9130	$1.0320 \times 10^{-7}$	0.0085
$w_{pA}$	0.1475	1.6794	0.0082	0.1962
$w_{bA}$	$8.8645 \times 10^{-10}$	$8.8645 \times 10^{-6}$	$7.4366 \times 10^{-16}$	$3.4419 \times 10^{-16}$
$\eta_{pA}$	0.6014	210.9814	0.0165	9.8958
$\eta_{bA}$	0	$2.1145 \times 10^{-35}$	0	0
$\eta_{p\tau}$	0.0079	$1.6818 \times 10^3$	$2.1660 \times 10^{-4}$	15.9581
$\eta_{b\tau}$	0	$2.1145 \times 10^{-31}$	0	0
$\eta_{e\tau}$	$6.8770 \times 10^{-11}$	$1.7706 \times 10^{-5}$	$2.5938 \times 10^{-16}$	$4.2568 \times 10^{-15}$

TABLE 4: Kinematic and dynamic coupling indexes with the fourth and seventh joints locked.

	Single	Local value Maximum	Minimum	Global value
$w_{eA}^{4,7lock}$	$3.2168 \times 10^{-18}$	$8.4015 \times 10^{-16}$	0	$7.4488 \times 10^{-35}$
$w_{pA}^{4,7lock}$	0.1338	2.0813	0.0025	0.1471
$w_{bA}^{4,7lock}$	$6.4487 \times 10^{-21}$	$7.3665 \times 10^{-18}$	0	$3.7389 \times 10^{-40}$
$\eta_{pA}^{4,7lock}$	0.5825	145.4495	0.0072	8.0662
$\eta_{bA}^{4,7lock}$	0	$1.2862 \times 10^{-36}$	0	0
$\eta_{p\tau}^{4,7lock}$	0.0078	968.7484	$1.2646 \times 10^{-4}$	13.3688
$\eta_{b\tau}^{4,7lock}$	0	$1.0415 \times 10^{-31}$	0	0
$\eta_{e\tau}^{4,7lock}$	$3.9886 \times 10^{-26}$	$1.1401 \times 10^{-14}$	$5.7742 \times 10^{-30}$	$6.0911 \times 10^{-34}$

zero. Taking  $K_D = 0.5$  and  $K_p = 0.1$ ,  $\ddot{\theta}_p$  and  $\theta_p$  are in Figure 12 and  $\theta_A$ ,  $\dot{\theta}_A$ , and  $\tau_A$  are in Figure 13.

Figure 12 shows that the passive joint is regulated to the desired angle at 28.1 s, and the active joint's motion and tor-

que are smooth in Figure 13. Thus, the passive joint regulating task is accomplished based on the control method. The PD controller above is only appropriate to the space manipulator with an accurate dynamic model. Considering model

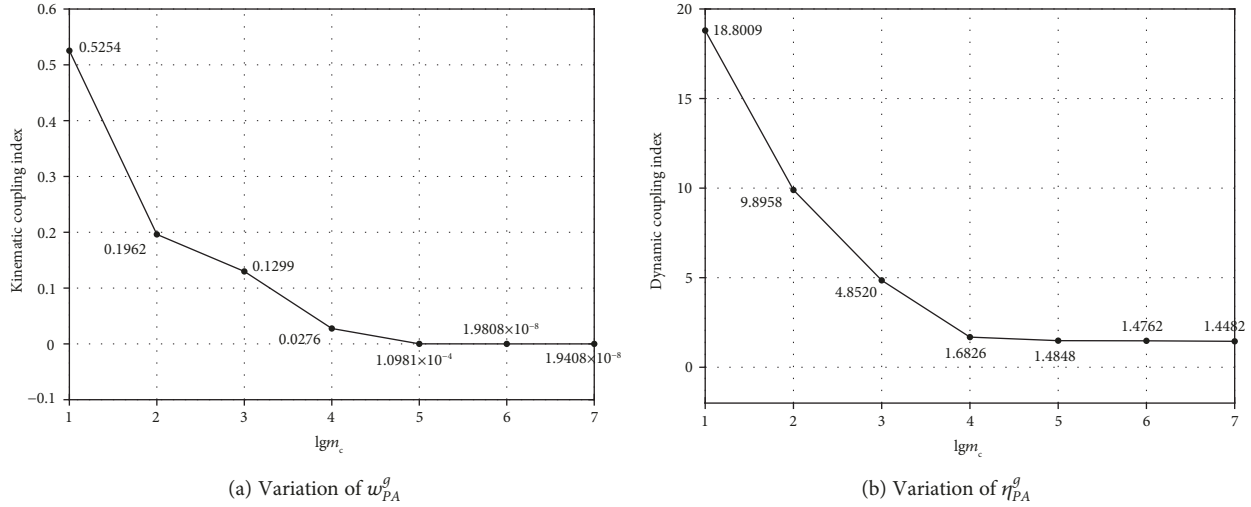


FIGURE 11: The variations of  $w_{PA}^g$  and  $\eta_{PA}^g$  with  $m_c$ .

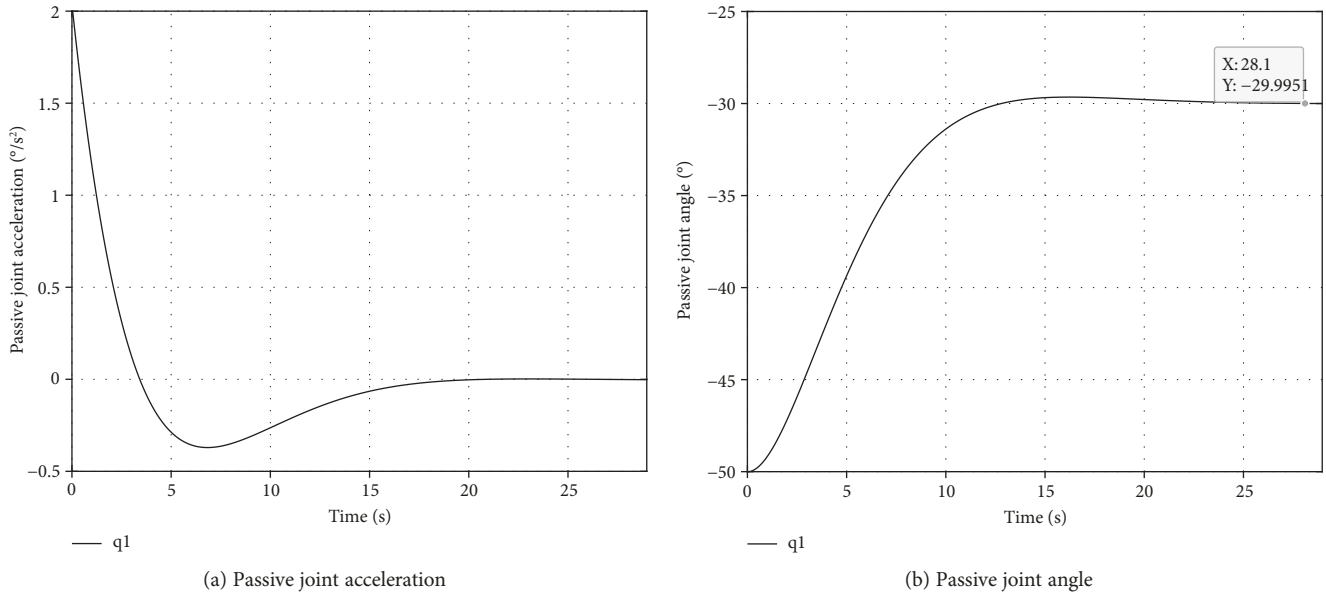


FIGURE 12: The motion of passive joints with the PD controller.

uncertainty and external disturbance, a robust control system needs to be designed. But in this paper, we mainly analyze the kinematic and dynamic characteristics of the space manipulator with free-swinging joint failure, instead of a robust controller design. In the future study, we will combine the sliding mode and fuzzy control method to design a controller robust to the bounded unknown disturbance and unmodeled uncertainty for the space manipulator with free-swinging joint failure.

The simulation above verifies the following theories:

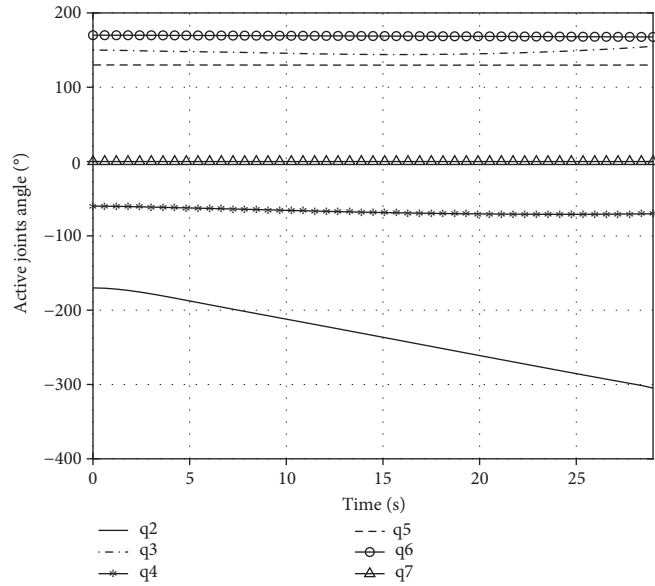
- (1) The first-order nonholonomic constraint and the second-order nonholonomic constraint do simultaneously exist inside the system of the space manipulator with free-swinging joint failure
- (2) The kinematic and dynamic coupling indexes proposed in this paper can objectively evaluate kinematic

and dynamic coupling degrees from active joints to passive units

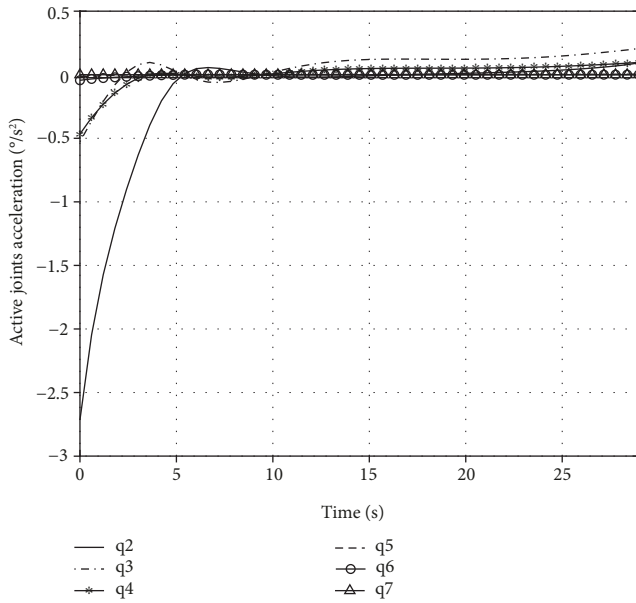
- (3) Many space tasks are either based on motion planning with the first-order nonholonomic constraint or based on a controller design with the second-order nonholonomic constraint

## 6. Conclusions

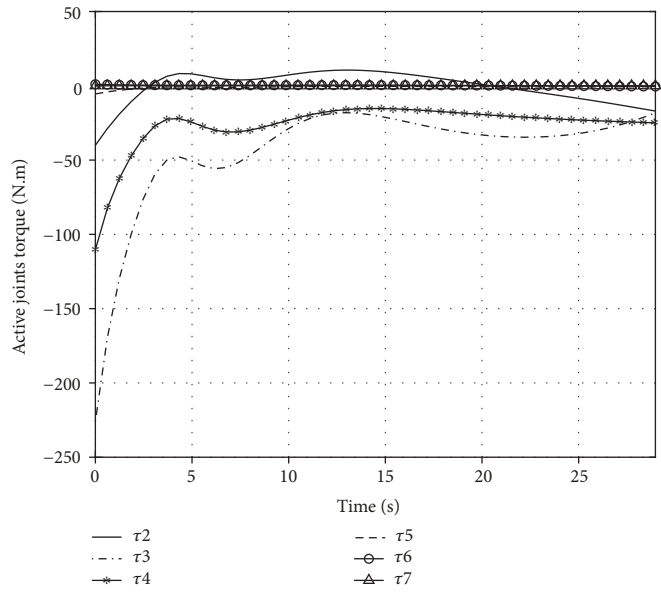
We analyze kinematic and dynamic characteristics of the free-floating space manipulators with free-swinging joint failure in this paper. Based on momentum conservation and the Lagrange equation, the kinematic and dynamic models are established. On this basis, the kinematic and dynamic coupling relationships are derived and we point out that the first-order nonholonomic constraint and the second-order nonholonomic constraint simultaneously exist



(a) Active joint angle



(b) Active joint acceleration



(c) Active joint torque

FIGURE 13: The variations of active joint motion and torque.

in the system. Local and global kinematic and dynamic coupling indexes are correspondingly defined. Finally, simulation experiments surrounding the SSRMS-type space manipulator are designed to verify the existence and correctness of the first-order and second-order nonholonomic constraints and display the execution effect of many tasks based on motion planning and the control method. The main contributions in this paper include the following:

- (1) We explicitly propose kinematic and dynamic modelling methods for the space manipulator with free-swinging joint failure for the first time
- (2) All kinematic coupling relationships (the first-order nonholonomic constraint) and dynamic coupling

relationships (the second-order nonholonomic constraint) inside the system of the space manipulator with free-swinging joint failure are derived

- (3) For general tasks, we propose the motion planning method based on the first-order nonholonomic constraint and design a control strategy based on the second-order nonholonomic constraint. This is the basis of treatment of free-swinging joint failure

In future research, we will pay more attention to task optimization to make the space manipulator with free-swinging joint failure perform primary and secondary tasks in the meantime. And we further design the control system to be robust to model uncertainty and external disturbance.

## Data Availability

The data and codes in MATLAB used to support the findings of this study are available from the corresponding author upon request.

## Conflicts of Interest

All authors declare that they have no conflicts of interest.

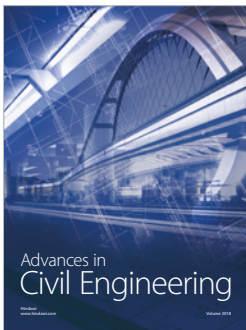
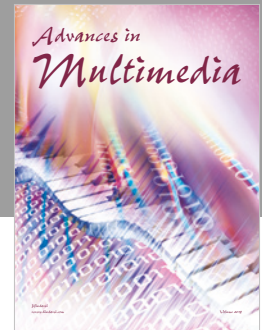
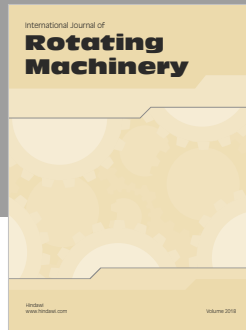
## Acknowledgments

This work was supported by the National Natural Science Foundation of China (61403038, 61573066) and Fundamental Research Funds for the Central Universities (2019PTB-012).

## References

- [1] B. Hu, F. Chen, L. Han, H. Chen, and H. Yu, "Design and ground verification of space station manipulator control method for orbital replacement unit changeout," *International Journal of Aerospace Engineering*, vol. 2018, Article ID 4271035, 18 pages, 2018.
- [2] P. Huang, L. Chen, B. Zhang, Z. Meng, and Z. Liu, "Autonomous rendezvous and docking with nonfull field of view for tethered space robot," *International Journal of Aerospace Engineering*, vol. 2017, Article ID 3162349, 11 pages, 2017.
- [3] G. Chen, B. Yuan, Q. Jia, H. Sun, and W. Guo, "Failure tolerance strategy of space manipulator for large load carrying tasks," *Acta Astronautica*, vol. 148, pp. 186–204, 2018.
- [4] R. S. Jamisola, A. A. Maciejewski, and R. G. Roberts, "Failure-tolerant path planning for kinematically redundant manipulators anticipating locked-joint failures," *IEEE Transactions on Robotics*, vol. 22, no. 4, pp. 603–612, 2006.
- [5] H. Abdi, S. Nahavandi, Y. Frayman, and A. A. Maciejewski, "Optimal mapping of joint faults into healthy joint velocity space for fault-tolerant redundant manipulators," *Robotica*, vol. 30, no. 4, pp. 635–648, 2012.
- [6] E. C. Wu, J. C. Hwang, and J. T. Chladek, "Fault-tolerant joint development for the space shuttle remote manipulator system: analysis and experiment," *IEEE Transactions on Robotics and Automation*, vol. 9, no. 5, pp. 675–684, 1993.
- [7] A. De Luca and R. Mattone, "Actuator failure detection and isolation using generalized momenta," in *2003 IEEE International Conference on Robotics and Automation (Cat. No. 03CH37422)*, pp. 634–639, Taipei, Taiwan, September 2003.
- [8] W. Guo, "Development of fault-tolerant motion control system for space manipulator with joint failure," Master Thesis, Beijing University of Posts and Telecommunications, Beijing, China, 2018.
- [9] Y. She, W. Xu, H. Su, B. Liang, and H. Shi, "Fault-tolerant analysis and control of SSRMS-type manipulators with single-joint failure," *Acta Astronautica*, vol. 120, pp. 270–286, 2016.
- [10] Q. Jia, T. Li, G. Chen, H. Sun, and J. Zhang, "Trajectory optimization for velocity jumps reduction considering the unexpectedness characteristics of space manipulator joint-locked failure," *International Journal of Aerospace Engineering*, vol. 2016, Article ID 7819540, 14 pages, 2016.
- [11] M. Hattori and H. Yabuno, "Reachable area of an underactuated space manipulator subjected to simple spinning," *Nonlinear Dynamics*, vol. 51, no. 1-2, pp. 345–353, 2008.
- [12] J. Shin and J. Lee, "Dynamic control of underactuated manipulators with free-swinging passive joints in Cartesian space," in *Proceedings of International Conference on Robotics and Automation*, pp. 3294–3299, Albuquerque, NM, USA, April 1997.
- [13] R. G. Roberts, "The dexterity and singularities of an underactuated robot," *Journal of Robotic Systems*, vol. 18, no. 4, pp. 159–169, 2001.
- [14] Y. Nakamura, T. Suzuki, and M. Koinuma, "Nonlinear behavior and control of a nonholonomic free-joint manipulator," *IEEE Transactions on Robotics and Automation*, vol. 13, no. 6, pp. 853–862, 1997.
- [15] H. Arai, K. Tanie, and N. Shiroma, "Nonholonomic control of a three-DOF planar underactuated manipulator," *IEEE Transactions on Robotics and Automation*, vol. 14, no. 5, pp. 681–695, 1998.
- [16] X.-Z. Lai, J. H. She, W. H. Cao, and S. X. Yang, "Stabilization of underactuated planar acrobot based on motion-state constraints," *International Journal of Non-Linear Mechanics*, vol. 77, pp. 342–347, 2015.
- [17] D. Liu, X. Lai, Y. Wang, X. Wan, and M. Wu, "Position control for planar four-link underactuated manipulator with a passive third joint," *ISA Transactions*, vol. 87, pp. 46–54, 2019.
- [18] X. Z. Lai, C. Z. Pan, M. Wu, S. X. Yang, and W. H. Cao, "Control of an underactuated three-link passive-active-active manipulator based on three stages and stability analysis," *Journal of Dynamic Systems, Measurement, and Control*, vol. 137, no. 2, article 021007, 2015.
- [19] X. Lai, P. Zhang, Y. Wang, and M. Wu, "Position-posture control of a planar four-link underactuated manipulator based on genetic algorithm," *IEEE Transactions on Industrial Electronics*, vol. 64, no. 6, pp. 4781–4791, 2017.
- [20] Y. Wang, X. Lai, L. Chen, H. Ding, and M. Wu, "A quick control strategy based on hybrid intelligent optimization algorithm for planar n-link underactuated manipulators," *Information Sciences*, vol. 420, pp. 148–158, 2017.
- [21] J. D. English and A. A. Maciejewski, "Measuring and reducing the Euclidean-space effects of robotic joint failures," *IEEE Transactions on Robotics and Automation*, vol. 16, no. 1, pp. 20–28, 2000.
- [22] M. Bergerman and Y. Xu, "Optimal control of manipulators with any number of passive joints," *Journal of Robotic Systems*, vol. 15, no. 3, pp. 115–129, 1998.
- [23] R. Mukherjee and Degang Chen, "Control of free-flying underactuated space manipulators to equilibrium manifolds," *IEEE Transactions on Robotics and Automation*, vol. 9, no. 5, pp. 561–570, 1993.
- [24] G. P. He, Z. Lu, and F. X. Wang, "Optimal control of underactuated redundant space-robot system," *Control Theory & Applications*, vol. 21, no. 2, pp. 305–310, 2004.
- [25] G. Chen, W. Guo, Q. Jia, X. Wang, and Y. Fu, "Failure treatment strategy and fault-tolerant path planning of a space manipulator with free-swinging joint failure," *Chinese Journal of Aeronautics*, vol. 31, no. 12, pp. 2290–2305, 2018.
- [26] X. H. Huang, Y. H. Jia, and S. J. Xu, "Path planning of a free-floating space robot based on the degree of controllability," *Science China Technological Sciences*, vol. 60, no. 2, pp. 251–263, 2017.

- [27] B. Liang, Y. Xu, and M. Bergerman, "Mapping a space manipulator to a dynamically equivalent manipulator," *Journal of Dynamic Systems Measurement and Control*, vol. 120, no. 1, pp. 1–7, 1998.
- [28] Y. Xie, X. Wu, T. Inamori, Z. Shi, X. Sun, and H. Cui, "Compensation of base disturbance using optimal trajectory planning of dual-manipulators in a space robot," *Advances in Space Research*, vol. 63, no. 3, pp. 1147–1160, 2019.
- [29] B. C. O. Maciel, M. H. Terra, and M. Bergerman, "Optimal robust control of underactuated manipulators via actuation redundancy," *Journal of Robotic Systems*, vol. 20, no. 11, pp. 635–648, 2003.
- [30] Q. Jia, Y. Liu, G. Chen, H. Sun, and J. Peng, "Analysis of load-carrying capacity for redundant free-floating space manipulators in trajectory tracking task," *Mathematical Problems in Engineering*, vol. 2014, Article ID 125940, 12 pages, 2014.



**Hindawi**

Submit your manuscripts at  
[www.hindawi.com](http://www.hindawi.com)

